

Hassan Naveed

# **CONTRIBUTION OF EXPOSED TIMBER TO FIRE LOAD**

A review of different calculation methods

Master's Thesis  
Faculty of Built Environment  
Examiner: Prof. Mikko Malaska  
Prof. Sami Pajunen  
May 2025

# ABSTRACT

Title : Contribution of Exposed Timber to Fire Load: A Review of Different Calculation Methods  
Author : Hassan Naveed  
Master's Thesis  
Tampere University  
Master's Degree Programme in Civil Engineering (Structural Engineering)  
May 2025

---

As the utilization of mass timber gains growing interest in modern architecture and construction, specifically the use of CLT and mass timber (Glulam, LVL, etc.), the importance of safe and reliable structural fire design is ever growing concern in modern fire safety principles. The emphasis on sustainability and low-carbon construction materials has led to an increase in the usage of exposed timber in modern construction. Unlike traditional design methods, the exposed timber surfaces contribute towards fire load and have considerable effects on fire growth, duration and decay. Therefore, adequate fire design methods are needed to ensure structural integrity, occupant safety and the utilization of exposed timber.

This thesis presents an empirical analysis of four design methods, FprEN 1995-1-2:2023, Brandon (2018a, 2018b), Xing et al. (2024) and Salminen and Hietaniemi (2017). The study is focused on the evaluation of key parameters like maximum fire temperature, time for maximum fire temperature, charring rate, charring depth and the fire load density, while utilizing the same compartment conditions for each design method.

The analysis was performed by calculating these key parameters using Mathcad software using parameters and equations, unique to each design method. The results provide a clear distinction between design methodology and design approach. Salminen and Hietaniemi (2017) provides the highest fire temperature but the shortest fire duration, with the highest charring rate among other methods, but lowest charring depth, emphasizing its utilization of thermodynamic heat transfer and ventilation parameters. Brandon (2018a, 2018b) and Xing et al. (2024) produced approximately similar fire duration and fire load, but Xing et al. (2024) adopts a more refined three stage fire model in its design methodology which led to lower maximum fire temperature and a slower charring rate compared to Brandon (2018a, 2018b). FprEN 1995-1-2:2023, while generally considered more conservative in its design methodology, provided intermediate results between all other methods. This can be contributed towards its more simplified and standardized design assumption rather than real-time development in the compartment.

The empirical analysis provides a key insight into the structural design process, that conservatism in the design approach is not always reflected in higher outputs, while it is based on the underlying assumptions that are utilized in the design methodology. The study concludes that the selection of design method for structural fire design should be based on the context of the design under consideration, material exposure and the intricate balance between ease of use, simplicity of the design process and safety achieved.

This study contributes to the continued development of performance based structural fire design practices for mass timber structures utilizing exposed structural elements and a detailed design approach is needed to study the contribution of this exposed structural timber in design methodology.

Keywords: Structural fire design, fire exposed mass timber, fire exposed CLT, fire load, charring rate, charring depth, fire safety.

The originality of this thesis has been checked using the Turnitin Originality Check service.

## USE OF AI IN THESIS

I have utilized AI tools in my thesis:

No

Yes

The AI tools utilized in my thesis and their purposes are described below:

Names and versions of AI tools: ChatGPT version 4.0 and Grammarly.

Purpose of using AI tools: The purpose of using AI tools was to improve understanding of certain concepts that were difficult to understand from the literature that is used in the research. AI tools were also used to improve the sentence structures and improve the readability of the text. ChatGPT version 4.0 was also utilized in the analysis of the calculation results to provide better understanding.

Sections where AI tools were used: ChatGPT version 4.0 was mostly used in Chapter 4 of this thesis, Analysis and Discussion, for aiding in understanding the output parameters and “Figure 7. *Compartment temperature vs. time curve for different calculation methods. (AI Generated)*” is generated using ChatGPT version 4.0. Grammarly was utilized throughout the thesis for checking grammar and spelling mistakes.

I acknowledge that I am fully responsible for the entire content of my thesis, including the parts generated by AI, and accept accountability for any violations of ethical standards in publications.

# PREFACE

Working on this thesis has been a delightful journey of my academic life. While this journey met with many challenges, there were also moments of learning, appreciation for the field of structural fire engineering and support from my teachers and classmates that I am truly grateful for.

Various people have made this achievement possible through their support and guidance. Especially my thesis supervisors Prof. Mikko Malaska, who despite his hectic schedule with performing and supervising fire tests and other teaching responsibilities, took time to guide and educate me throughout this master's thesis. Working with him has been a great experience. I would also like to thank my co-supervisor, Prof. Sami Pajunen for his continued collaboration with Prof. Mikko Malaska to steer this thesis process to its completion. I would also like to thank Mika Alanen for providing the necessary breakthrough for calculations.

A heartfelt thanks to my cousins Ali Nadeem and Haider Nadeem who have been my inspiration for coming to Finland to pursue a master's degree. Thank you for providing support when I needed it the most. Also, thanks to my parents for believing in me and keeping me in their prayers.

I hope that this research will contribute to the development of the field of structural fire design by providing insight in terms of use of exposed mass timber and CLT in construction.

Finally, I would like to thank my classmates, Mahlet, Ahtesham, Damsha, Gayan and Shan for providing their support throughout this academic journey and making this time memorable and enjoyable.

Tampere, 27 May 2025

Hassan Naveed

# CONTENTS

1. INTRODUCTION.....	1
1.1 Background.....	1
1.2 Objectives.....	3
2. THEORITICAL BACKGROUND.....	5
2.1 Brandon (2016).....	8
2.2 Brandon (2018a, 2018b).....	10
2.3 Salminen and Hietaniemi (2017).....	13
2.4 FprEN 1995-1-2:2023.....	15
2.5 Xing et al. (2024).....	17
2.6 Summary.....	18
3. CALCULATIONS AND RESULTS.....	20
3.1 Compartment Details.....	20
3.2 Calculation Methodology.....	21
3.3 Brandon (2016).....	22
3.4 FprEN 1995-1-2:2023.....	23
3.5 Brandon (2018a, 2018b).....	26
3.6 Xing et al. (2024).....	28
3.7 Salminen and Hietaniemi (2017).....	30
3.8 Summary of Results.....	32
4. ANALYSIS AND DISCUSSION.....	35
4.1 Introduction.....	35
4.2 Difference in Output Parameters.....	35
4.2.1 FprEN 1995-1-2:2023.....	35
4.2.2 Brandon (2018a, 2018b).....	36
4.2.3 Xing et al. (2024).....	36
4.2.4 Salminen and Hietaniemi (2017).....	36
4.3 Methodological Framework.....	37
4.3.1 FprEN 1995-1-2:2023.....	37
4.3.2 Brandon (2018a, 2018b).....	37
4.3.3 Xing et al. (2024).....	38
4.3.4 Salminen and Hietaniemi (2017).....	38

4.4	Reasons for Divergence in Results .....	39
4.5	Exposed Mass Timber vs. CLT .....	40
4.6	Area of Exposed Timber vs. Fire Load .....	41
4.7	Exposed Timber vs. Decay Phase .....	42
5.	CONCLUSION .....	44
5.1	Results.....	44
5.2	Further Research.....	45
	REFERENCES.....	46
	Appendix A: Calculations EN-1991-1-2-2023 .....	49
	Appendix B: Calculations Brandon (2018).....	62
	Appendix C: Calculations Xing et al. (2024) .....	70
	Appendix D: Calculations Salminen and Heitaniemi (2017).....	73

## LIST OF FIGURES

<b>Figure 1.</b>	<i>Effective Cross Section according to RCSM (Brandon, 2016) .....</i>	<i>3</i>
<b>Figure 2.</b>	<i>Algorithm for the SP-TimFire (Brandon, 2016).....</i>	<i>8</i>
<b>Figure 3.</b>	<i>Comparison of maximum charring depths from experimental results and calculated predictions (Brandon, 2018b). .....</i>	<i>12</i>
<b>Figure 4.</b>	<i>Basic idea of quantitative risk analysis for fire design (Salminen and Hietaniemi, 2017) . .....</i>	<i>13</i>
<b>Figure 5.</b>	<i>Compartment plan used to perform calculations for different methods. </i>	<i>20</i>
<b>Figure 6.</b>	<i>Comparison between <math>t_o</math> and <math>\beta_o</math>. .....</i>	<i>24</i>
<b>Figure 7.</b>	<i>Compartment temperature vs. time curve for different calculation methods (AI Generated) .....</i>	<i>33</i>
<b>Figure 8.</b>	<i>Comparison of charring depths determined by different calculation methods .....</i>	<i>34</i>
<b>Figure 9.</b>	<i>Comparison of charring rates determined by different calculation methods .....</i>	<i>34</i>

## LIST OF TABLES

<b>Table 1.</b>	<i>Comparison of different calculation methods.....</i>	<i>19</i>
<b>Table 2.</b>	<i>Input parameters and related equations in the FprEN 1995-1-2:2023 method.....</i>	<i>25</i>
<b>Table 3.</b>	<i>Output parameters and related equations in the FprEN 1995-1-2:2023 method.....</i>	<i>26</i>
<b>Table 4.</b>	<i>Input parameters and related equations in the Brandon (2018a, 2018b) method.....</i>	<i>27</i>
<b>Table 5.</b>	<i>Output parameters and related equations in the Brandon (2018a, 2018b) method.....</i>	<i>28</i>
<b>Table 6.</b>	<i>Input parameters and related equations in the Xing et al. (2024) method.....</i>	<i>29</i>
<b>Table 7.</b>	<i>Output parameters and related equations in the Xing et al. (2024) method.....</i>	<i>29</i>
<b>Table 8.</b>	<i>Input parameters and related equations in the Salminen and Heitaniemi (2017) method.....</i>	<i>30</i>
<b>Table 9.</b>	<i>Output parameters and related equations in the Salminen and Heitaniemi (2017) method.....</i>	<i>32</i>
<b>Table 10.</b>	<i>Compilation of results from calculation methods.....</i>	<i>32</i>
<b>Table 11.</b>	<i>Comparison of output parameters according to FprEN 1995-1-2:2023 calculations when one wall and four walls are exposed to fire .....</i>	<i>41</i>

## LIST OF SYMBOLS AND ABBREVIATIONS

CLT	Cross Laminated Timber
HRR	Heat Release Rate
LVL	Laminated Veneer Lumber
RCSM	Reduced Cross Section Method

$A$	Area of Opening [ $m^2$ ]
$A_v$	Area of Ventilation [ $m^2$ ]
$A_t$	Total Surface Area [ $m^2$ ]
$A_f$	Floor Area [ $m^2$ ]
$A_{CLT}$	Area of exposed CLT [ $m^2$ ]
$A_{st}$	Area of Combusting Surfaces [ $m^2$ ]
$A_{prot}$	Area of Protected Surfaces [ $m^2$ ]
$A_w$	Area of Windows [ $m^2$ ]
$A_{fz}$	Area of Fire [ $m^2$ ]
$a$	Empirical Factor, Dimensionless
$c$	Specific Heat of Air [ $J/kgK$ ]
$c_1$	Specific Heat of Wood [ $J/kgK$ ]
$c_2$	Specific Heat of Gypsum [ $J/kgK$ ]
$c_g$	Specific Heat of Air [ $J/kgK$ ]
$d_{char}$	Char Depth [ $mm$ ]
$exp$	Percentage of Exposed Area, Dimensionless
$G_o$	Mass of CLT [ $kg$ ]
$g$	Acceleration due to Gravity [ $m/s^2$ ]
$h$	Height of Opening [ $m$ ]
$h_{eq}$	Height of Opening [ $m$ ]
$h_v$	Height of Ventilation [ $m$ ]
$k_h$	Empirical Factor, Dimensionless

$k_p$	Empirical Factor, Dimensionless
$k_c$	Thermal Conductivity of Lining Material [ $J/msK$ ]
$k_d$	Thermal Diffusivity of Lining Material [ $m^2/s$ ]
$l$	Flame Height [ $m$ ]
$m$	Combustion Factor, Dimensionless
$O$	Opening Factor [ $m^{1/2}$ ]
$Q_c$	HRR due to moveable fire load [ $MJ/s$ ]
$Q_{c:CLT}$	Assumed HRR for CLT [ $MJ/m^2mm$ ]
$Q_{c:max}$	Maximum HRR in the compartment [ $MJ m^3/kg$ ]
$Q_w$	Rate of heat loss through compartment boundaries [ $MJ/s$ ]
$Q_R$	Loss of radiant heat through compartment openings [ $MJ/s$ ]
$Q_L$	Rate of heat loss due to air escape [ $MJ m^3/kg$ ]
$q_{mfl}$	Moveable Fire Load Density [ $MJ/m^2$ ]
$q_{td}$	Fire Load Density [ $MJ/m^2$ ]
$q_{td:max}$	Maximum Fire Load Density [ $MJ/m^2$ ]
$q_{d;fi;t}$	Fire Load Density Related to Floor Area [ $MJ/m^2$ ]
$q_{d;fi}$	Design Value of Fire Load Density [ $MJ/m^2$ ]
$q_{d;st;t}$	Structural Fire Load Density [ $MJ/m^2$ ]
$q_{d;total;t}$	Total Fire Load Density [ $MJ/m^2$ ]
$q_E$	Net Heat Flux [ $J/m^2s$ ]
$R$	Rate of change of fuel mass [ $kg/s$ ]
$s_{10}$	Empirical Factor [ $MW/m^2$ ]
$T_{max}$	Assumed Maximum Fire Temperature [ $K$ ]
$T_f$	Fire Temperature in compartment [ $K$ ]
$T_{\infty}$	Ambient Temperature in compartment [ $K$ ]
$T_g$	Fire Temperature [ $^{\circ}C$ ]
$T_o$	Ambient Temperature [ $^{\circ}C$ ]
$Ther_{par}$	Weighted area in exposed surface and gypsum, Dimensionless
$t_o$	Time for constant charring rate [ $min$ ]

$t_{lim}$	Limiting Time for fire [h]
$t_{max}$	Maximum Time fir Heat Phase [min]
$U_a$	Flow rate of air [kg/s]
$\alpha$	Empirical Factor, Dimensionless
$\alpha_1$	Flow constant for fires, Dimensionless
$\alpha_1$	Correction factor for boundary condition [MJ/m <sup>2</sup> mm]
$\alpha_{st}$	Empirical Factor, Dimensionless
$\beta$	Empirical Factor, Dimensionless
$\beta_{exp}$	Percentage rise of charring rate to exposed area, Dimensionless
$\beta_o$	One-Dimensional charring rate [mm/min]
$\beta_n$	Nominal Charring Rate [mm/min]
$\beta_{par}$	Parametric Charring Rate [mm/min]
$\rho$	Density of Air [kg/m <sup>3</sup> ]
$\rho_1$	Density of Wood [kg/m <sup>3</sup> ]
$\rho_2$	Density of Gypsum [kg/m <sup>3</sup> ]
$\Gamma$	Heat Rate Factor, Dimensionless
$\lambda_1$	Thermal Conductivity of Wood [W/mK]
$\lambda_2$	Thermal Conductivity of Gypsum [W/mK]
$\phi$	Ventilation Parameter [kg/s]
$\zeta$	Empirical Factor, Dimensionless
$\eta$	Empirical Factor, Dimensionless
$\sigma$	Stefan Boltzmann Constant
$\tau$	Time of Primary Burning [s]
$\Omega$	Empirical Factor, Dimensionless
$\Theta_{max}$	Maximum Fire Temperature [°C]
$\Delta H_c$	Heat of combustion of charr layer [J/kg]
$\Delta H_v$	Heat of combustion of volatile gases [J/kg]

# 1. INTRODUCTION

## 1.1 Background

Wood has emerged as one of the most versatile materials to be used in the construction industry in recent years. Some of the qualities of wood that make it a desirable material are that its light weight compared to other conventional construction materials like stone, bricks or concrete but possesses comparable strength to these materials (Švajlenka & Pošiváková, 2023). The workability and ease of manufacturing of wood is also a factor that makes it easier to use in a variety of residential and commercial buildings and structures. The advancement in the production of engineered timber products has also played a vital role in the resurgence of wood as a construction material in the present day and age where more focus is put forward in making the construction industry more sustainable as 40% of the global carbon dioxide emissions are related to the construction industry (Kamyab et al., 2020).

The shift towards traditional and sustainable wood-based construction has been on the rise around the world. Wood has already been used as a traditional construction material in houses and offices, but concrete and steel has always been the dominating construction material in urban infrastructure and multi-storey buildings. But this trend is changing with more timber multi-storey buildings on the rise (Gosselin et al., 2016). In recent years, timber construction has increased its market share through growing interest in multi-storey timber construction and massive engineered timber products. From an architectural perspective, the use of wood is a matter of expression and aesthetics. In the context of Finland, whether it is urban infrastructure or houses, the customers appreciate the ecological, aesthetic, comforting and appealing nature of wood as a construction material (Viholainen et al., 2020).

The wood or more technically referred to as timber in the literature, has been used in many ways when it comes to construction material. The most popular engineered timber products that are being used for construction are plywood, laminated veneer lumber (LVL), cross laminated timber (CLT), glued laminated timber and different structural members like beams, columns, ceilings,

floor members and ceilings (Yadav & Kumar, 2022). When using these engineered timber products, the surface of the products can be exposed, or it can be treated with chemicals or fire-retardant materials to protect it from fire. This is highly subjective to the intended use and purpose of the construction. For this study the role of unprotected timber is being considered.

The concept of unprotected timber is that the timber products or structural members that are used in the infrastructure are untreated, and the surface of the structural members is exposed. The use of exposed timber in multi-storey buildings is limited due to the combustible nature of the material (Menis et al., 2019). With the increased use of exposed timber in construction, more robust design parameters are needed to be utilized to promote the fire safety of timber construction. The problem that exposed timber poses when it comes to fire safety is that the exposed surfaces increase the fire load during the combustion phase in fire development. This may lead to rapid development of fire that is not desirable where the safety of the occupants is concerned.

The fire safety in timber construction is a topic that has captivated the interest of researchers for many years. The main challenges that timber products possess, when it comes to fire safety is the unpredictability of material. There are many uncertainties that come into play during a fire including the nature and composition of the material and loads on the structure and predicting the behavior of wood is a challenging task. Designers often struggle to predict the safety risks associated with timber construction due to the lack of knowledge of the fire performance of engineered timber products (Richter et al., 2020).

For predicting the behavior of exposed timber, the methods range from simpler to advanced. In the simpler methods, to calculate the fire resistance, either reduced cross section method or reduced properties method is considered. In reduced cross section method, the reduction in the cross section of the timber element is predicted by measuring the char depth and the fire resistance is predicted using the residual cross section. In the reduced properties method, the influence of internal temperature on the mechanical properties of the timber is also considered. On the contrary, in advanced methods, finite element modeling and thermomechanical behavior of timber are the basis for fire resistance determination (Marcolan Júnior & Dias de Moraes, 2018).

Eurocode 5 provides guidelines for the fire design of exposed timber. The most important parameters in this regard are fire load and char depth. Fire load has the main contribution in the heat releasing rate and it is the sum of all the combustible material present inside a space and it

is expressed as  $\text{MJ}/\text{m}^2$  (Dundar & Selamat, 2023). The char depth is the thickness of the char layer that develops on the surface of the timber exposed to fire (Suzanne et al., 2023). As the char depth increases, the load bearing capacity of the timber member reduces. Current Eurocode 5 (EN 1995-1-2:2004) does not provide guidelines for determining the contribution of exposed timber to fire load. However, a method will be included in the next generation of the standard. This study examines the calculation method included in the new version of the standard.

The method that Eurocode 5 provides for the determination of structural fire resistance, which is the time taken by the members to maintain the structural integrity before failure, is Reduced Cross Section Method (RCSM). In the method, the charring layer and zero-strength layer is subtracted to find an effective cross section that will be able to bear the loads. There are differences between this method and the experimental data that is obtained by performing different fire tests (Brandon, 2016).

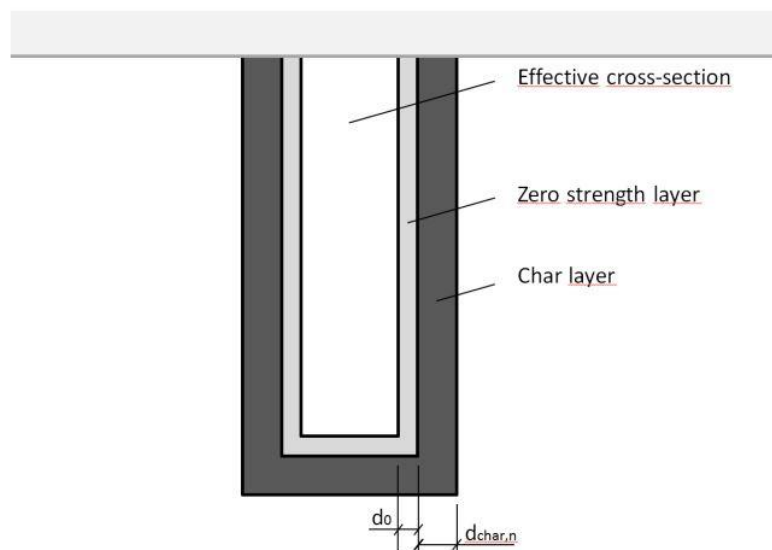


**Figure 1.** Effective cross section according to RCSM (Brandon, 2016).

## 1.2 Objectives

There are a variety of calculation methods that are being used to determine the contribution of structural timber to the rate of heat release, fire load, fire temperature, charring rate and charring depth. The problem that arises with these calculation methods is that every method provides different guidelines and parameters for fire design. These methods are based on fire tests

performed on different exposed timber members. There are many uncertainties that may arise due to the composition of the timber members used, the parameters of fire used in these experiments and the experimental setup. The applicability of the results from these experimental methods is also an issue because the results may not be applicable to bigger compartment sizes.

This thesis aims to study all four of these methods and provide a comparative study to determine the applicability of these different methods. The Arup Guide “Fire Safe Design of Mass Timber Buildings” is the driving force behind this research. In this guide, there are different calculation methods that are mentioned which are used for the fire design of exposed timber. The focus of this thesis is to study these methods by performing calculations using a standard compartment size. The objective of this study is to determine the usability of different design methods when the structural fire design of exposed mass timber structures is concerned.

The results obtained from the calculations will be analyzed to provide comparisons between different calculation methodologies. The results from this research will provide understanding of the fire safety design of exposed timber structures and the differences in the design approach and parameters. This study aims to answer the following questions:

- How does the area of exposed mass timber affect the availability of fuel load during the progression of fire in the compartment?
- How does exposed mass timber affect the decay phase of fire?
- How to estimate/ determine the char depth and combustible fire load, considering the involvement of exposed mass timber?
- Can the same methods be applied in the case of Cross-Laminated Timber (CLT)? What are the issues or differences that are needed to be addressed in this case?

## 2. THEORITICAL BACKGROUND

To increase the understanding regarding the contribution of exposed timber in fire load, studying the effects that timber has on the heat release rate (HRR) and fire temperatures is essential. The heat release rate (HRR) is the measurement of the amount of energy that is released per unit time, from the combustion of timber. HRR is crucial for understanding different properties and behavior of timber under fire which include fire growth, intensity of the fire and the potential for flashover (Aseeva et al., 2013).

Girompaire and Dagenais (2024) in their study to determine the heat release rate in exposed compartmental fires utilizing mass timber structural elements, used a two-zone model approach to estimate the HRR. The formulas from their study are given below (Girompaire and Dagenais, 2024):

The formula for HRR as a varying fuel load is provided as (Girompaire and Dagenais, 2024):

$$Q(t) = \alpha \cdot t^2 \quad (1)$$

Where  $\alpha$  is the fire growth rate measured in  $\text{kW/s}^2$  and time  $t$  ranges from 0 to  $t_{max}$ , the time taken to achieve the maximum fire temperature.

The study further provides formulas for heat release rates when discussing fully developed fire, ventilation-controlled fire and fuel-controlled fire. These will be discussed in detail later in this chapter when the calculation methods will be discussed.

HRR in timber can be influenced by certain factors that include:

- **Moisture Content:** Moisture content has an inverse correlation with HRR. Timber having greater moisture content exhausts more energy for evaporation which delays the ignition process and reduces the HRR. On the contrary, a dried-out timber having a lower moisture content leads to faster ignition and higher HRR (Bartlett et al., 2018).
- **Specific Species and Wood Density:** Denser wood species provide more fuel load for combustion, which in turn leads to more HRR. Wood species and cell structures in timber, therefore, play a crucial role in influencing the HRR (Tran and White, 1992).

- **External Heat Flux:** The influence of radiant heat also influences the HRR in timber. Higher heat flux increases the rate of pyrolysis and combustion, which increases the HRR (Aseeva et al., 2013).
- **Char Layer:** The formation of char layer can also influence the HRR. The formation of char layer on the surface of the timber during combustion serves as an insulation, which decreases the heat penetration and reduces the HRR. Wood density and specific species have varying effects in this phenomenon (Bartlett et al., 2018).
- **Surface Area and Dimensions of Timber:** The shape and size of the timber members under pyrolysis can influence the HRR. Generally, greater surface areas lead to increased HRR, while greater cross-sectional areas lead to reduced HRR (Fonseca & Barreira, 2009).
- **Ventilation and Oxygen Availability:** The availability of oxygen during the combustion process influences the HRR. Lower oxygen levels lead to incomplete combustion of timber which decreases the HRR. On the contrary, higher oxygen levels and adequate ventilation promote higher HRR (Bartlett et al., 2018).

When considering the use of exposed timber in construction, the influence of exposed timber on the fire temperature is an important aspect in fire design. Timber is a combustible material that can have considerable impact on the duration and intensity of the fire which leads to the need to understand the influence of timber on fire temperatures in compartment fires. Timber can influence the fire temperature in the following ways:

- **Temperature and Fire Intensity:** The correlation between HRR and fire temperature is linked with exposed timber. The exposed timber increases the HRR, which in turn leads to higher compartmental temperatures. This phenomenon is influenced by several factors including the surface area, the density and species of timber and the oxygen level and ventilation conditions (Ni and Gernay, 2022). The study by Ni and Gernay (2022) provides considerable information about the influence of exposed timber in compartment fires, which makes it critical to estimate the design fires accurately.
- **Charring Rate and Thermal Degradation:** During the combustion process, the timber develops a char layer that acts as an insulator layer and influences fire temperatures. Khelifa et al. (2024) studied the variation in thermo-physical properties and the development of char layer, providing insight into this aspect. The simulations performed during this study suggest that the fire temperatures increase with the duration of the fire,

before the formation of new char layers leaves the timber members structurally weaker due to char layer fall off. (Khelifa et al., 2024).

- **Oxygen Availability:** The availability of oxygen influences the fire temperature in a similar manner to the HRR. Frangi and Fontana (2005) studied the behavior of timber under natural fire conditions. The experiment suggested that the fire temperatures near the openings were considerably higher compared to the areas farthest from the openings. This gives the idea that oxygen levels increase pyrolysis and increase the fire temperature (Frangi and Fontana, 2005).
- **Timber Connections:** The type of connections that are used can also change the heat transfer profile in timber members. Maraveas et al. (2013) conducted a study to observe the behavior of different timber connections under fire. The studies concluded that timber connection failures are directly related to the temperature profiles around the connections. Thin connectors like nails and screws under fire, fail due to loss of yield strength. For larger connectors like fasteners and bolts, charring occurs around them at elevated temperatures, which reduces the bearing strength of the wood around these connectors and leads to rapid failure. This study gives an idea about how different connectors can influence the heat transfer rate and fire temperature (Maraveas et al., 2013).

Following the discussion regarding the influence of exposed timber on HRR and fire temperatures, the literature review will explore different calculation methodologies that are used to estimate different parameters including the ones mentioned above. The literature review will provide in-depth analysis of the following methodologies mentioned in different research papers:

- “Practical method to determine the contribution of structural timber to the rate of heat release and fire temperature of post-flashover compartment fires” (Brandon, 2016).
- “Engineering methods for structural fire design of wood buildings– Structural integrity during a full natural fire” (Brandon, 2018a, 2018b).
- “Performance-Based Fire Design of 14-Story Residential Mass Timber Building” (Salminen and Hietaniemi, 2017)
- “FprEN 1995-1-2:2023: Eurocode 5 - Design of timber structures - Part 1-2: Structural fire design”
- “Theoretical model of the three - Stage parameter fire curve considering the contribution of combustible materials” (Xing et al., 2024).

## 2.1 Brandon (2016)

The primary objective of this study conducted by Brandon (2016) was the estimation of the contribution of exposed timber and protected timber in compartment fires, with primary focus on the post-flashover phase, for a floor area of up to  $100 \text{ m}^2$ . For this estimation, Brandon (2016) introduced the model “SP-TimFire”. This model is a combination of a one-zone model and wood combustion model. The algorithm of the model is presented in Figure 2 below:

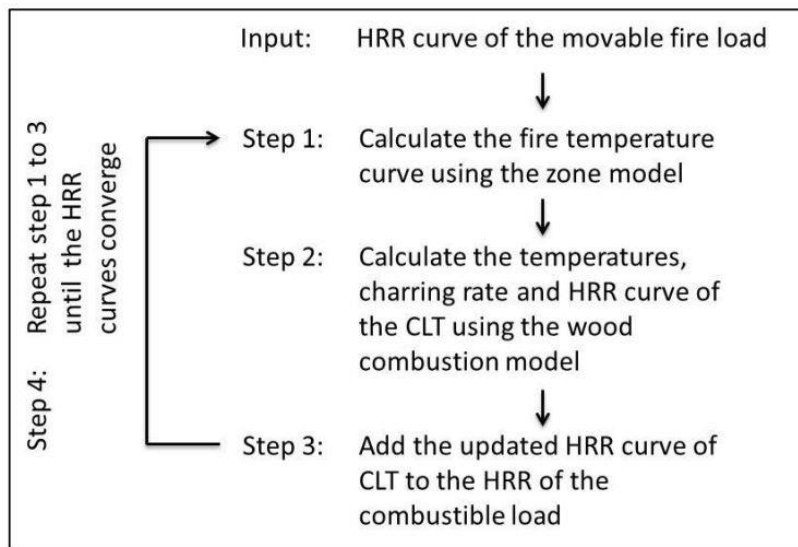


**Figure 2.** Algorithm for the SP-TimFire (Brandon, 2016).

Step 1 uses the one-zone model for calculating the fire temperature using HRR of the CLT (Cross-Laminated Timber) and moveable fire load.

Step 2 uses wood combustion model to calculate the HRR for CLT walls and ceilings from the fire temperature. These temperatures are exclusively based on the fire temperatures. The assumptions used for simplification state that the oxygen level and velocity of the air does not have any influence on the charring rate. The charring temperature of  $300^\circ \text{ C}$  and heat release per charring depth of  $5.39 \text{ MJ}/\text{m}^2\text{mm}$  is used to estimate the charring rate and HRR/unit area.

Step 3 uses the following assumption to update the HRR curves for iterations in the algorithm: “The heat release rate of the fire is assumed to be equal to the heat release rate of the CLT plus the heat release rate of the movable fire load” (Brandon, 2016). This assumption is later explained in the form of curves that provide a comparison between experimentally determined and predicted HRR.

For a brief discussion on the one-zone model, the main goal of this model is the determination of fire temperatures from HRR curves. The first model was introduced in 1970 which was developed based on conservation of energy and mass, and it was further developed for parametric fire curves in Eurocode 1.

For an under-ventilated fire, the HRR is given by the following equation (Brandon, 2016):

$$\min(Q_C + Q_{C;CLT} ; Q_{C;max}) = Q_w + Q_R + Q_L \quad (2)$$

In equation (2),  $Q_C$  is the HRR due to moveable fire load in the compartment,  $Q_{C;CLT}$  is the HRR due to combustible CLT structural members in the compartment, at the start of the iterations, this value is taken as  $5.39 \text{ MJ}/\text{m}^2\text{mm}$  as mentioned above and for the second iteration this value is multiplied by the charr depth calculated in the first iteration and  $Q_{C;max}$  is the maximum HRR inside the compartment and it is determined from the following equation (Brandon, 2016):

$$Q_{C;max} = \alpha_1 T_{max} c A \sqrt{h} \quad (3)$$

Where  $\alpha_1$  is a flow constant,  $T_{max}$  is the theoretical maximum fire temperature proposed as 1325 K (Wickström, 1986),  $c$  is the specific heat of air,  $A$  is the area of the opening in the compartment and,  $h$  is the height of the opening (Brandon, 2016).

$Q_w$  is the rate of heat loss through compartment boundaries.

$Q_L$  is the rate of heat loss due to the air escaping from the openings in the compartment and can be calculated from the following equation (Brandon, 2016):

$$Q_L = \alpha_1 (T_f - T_\infty) c A \sqrt{h} \quad (4)$$

Where  $T_f$  is the fire temperature in the compartment in K and  $T_\infty$  is the ambient temperature in the compartment in K.

$Q_R$  is the HRR that represents the loss of radiant heat from the compartment openings and is calculated by using the following equation (Brandon, 2016):

$$Q_R = A (T_f^4 - T_\infty^4) \sigma \quad (5)$$

Where  $\sigma$  is Stefan Boltzmann constant.

To determine the fire temperature  $T_f$ , equation (4) is substituted in equation (2) and rearranged to get the following equation for  $T_f$  (Brandon, 2016):

$$T_f = \frac{\min(Q_C + Q_{C,CLT}; Q_{C,max}) - Q_w - Q_R}{\alpha_1 c A \sqrt{h}} + T_\infty \quad (6)$$

To make the results of this algorithm more comparable with the actual compartment fire tests, several assumptions were made to achieve the desired outcome. The following conclusions have been presented by Brandon (2016) based on a comparison between experimental fire test results performed by McGregor (2013) and Medina and Hevia (2014), and the results obtained by using the SP-TimFire algorithm (Brandon, 2016):

- If the role of delamination of CLT is considered in case of fully exposed compartment surfaces, the decay phase of the fire is not predicted during the timeframe of the fire test, before the fire is manually extinguished, which indicates that the temperatures are expected to rise slowly during the fire test. On the other hand, if delamination is not considered, the SP-TimFire algorithm predicts the decay phase to commence during the timeframe of the fire test. However, this is not happening in the actual fire tests performed (Brandon, 2016).
- The other comparison states the overestimation of HRR after flashover and delamination. This happens due to the assumption on which the algorithm is based that states that all the delamination that happens in CLT is happening at the same time. Practically, this is not true as the heat or fire that is burning the CLT during fire testing may or may not be constant. This issue can be corrected by using multiple heat transfer models that measure delamination at different points of CLT.
- This method estimates compartment temperatures considerably accurate, when only one compartment wall is exposed to fire and the other surfaces in the compartment are protected and the char fall-off and delamination do not occur.
- When more than one compartment wall is exposed, the method determines the start of the decay phase satisfactorily but underestimates the temperatures.

## 2.2 Brandon (2018a, 2018b)

This calculation method is based exclusively on unconventional mass timber buildings that refer to buildings that are more than 16 story timber buildings. The nature of the failure is referred to as a progressive failure, meaning that in case of a fire, one timber member may lose its strength and then lead to failure of multiple members. This phenomenon has grave consequences for the life of the occupants in the building and severe financial implications. The design philosophy in such

cases is based on a compartmental fire design which involves a decay phase and self-extinguishment in case of a fully developed fire.

As it is not possible to test such a building under natural fire conditions, analytical design approach is used to numerically simulate the fire conditions to test the performance of the building. The analytical design is based on parametric design fires which involve a fully developed phase and a decay phase. Second flashover is not considered in parametric design fires, but practically it can happen, due to the delamination in case of CLT and the failure of protective layers for fire retardation like gypsum sheets.

For the parametric design fires, emphasis is done on the estimation of fuel load. It is not possible to directly calculate the influence of exposed timber in fuel load. One method to make the exposed timber resist the influence of fire is to use adhesives and fasteners that eliminate the delamination during fire.

To calculate the involvement of exposed timber in the fuel load  $q_{td}$  during the progression of fire, Brandon (2018a, 2018b), proposed an iterative method using the following equation (Brandon, 2018a):

$$q_{td}^{i+1} = q_{mfl} + \frac{A_{CLT} \cdot \alpha_1 \cdot (d_{char;end}^i)^{-0.7} \cdot \beta_{par} \cdot t_{max}^1}{A_c} \quad (7)$$

In equation (7),  $q_{mfl}$  represents the fire load density in the compartment given in  $MJ/m^2$ , due to moveable fire load and can be determined using Table E.5, EN 1991-1-2-2002, or using the values used in the other research literature. For this study, the value was taken from (Buchanan & Östman, 2022).

$A_{CLT}$  is the area of exposed CLT in the compartment given in  $m^2$  and can be determined directly from the compartment dimensions.

$\alpha_1$  is the correction factor proposed by (Buchanan & Östman, 2022) for the boundary conditions in the compartment and the value is equal to  $5.39 MJ/m^2mm$ .

$d_{char;end}^i$  is the charring depth given in  $mm$  and can be calculated using the following equation (Brandon, 2018b, Equation 13):

$$d_{char;end} = 2 \cdot \beta_{par} \cdot t_o \quad (8)$$

Where  $\beta_{par}$  is the parametric charring rate in  $mm/min$  calculated using Brandon (2018b), Equation 9 and  $t_o$  is the time in  $min$ , at which the charring rate becomes constant and can be calculated using Brandon (2018b), Equation 10.

$t_{max}^1$  is the duration of the heating phase of fire in  $h$ , that in which the maximum fire temperature will be attained and this can be calculated from the following equation (Brandon, 2018b):

$$t_{max} = \max [(0.2 \times 10^{-3} q_{td} / 0); t_{lim}] \quad (9)$$

Brandon (2018a, 2018b) method is an iterative method in which the char depth is the only input parameter that is changing in the subsequent iterations, while all the other parameters remain constant. At each iteration, the charring depth from the first iteration is used to determine the fuel load in the second iteration and the process is repeated until the difference between the charring depth in subsequent iterations becomes 0.1%, at which point the iterations can be stopped.

There are many factors associated with exposed timber that can complicate the calculations. The comparison between larger and smaller portions of exposed timber showed approximately similar fire temperatures during the fully developed fire phase. The comparison between predicted charring depths and actual experimental charring depths shows that the iterative method gives more conservative values. This indicates that the conservative parametric design fires can be used to predict the structural integrity and failure of the structures with exposed timber surfaces.

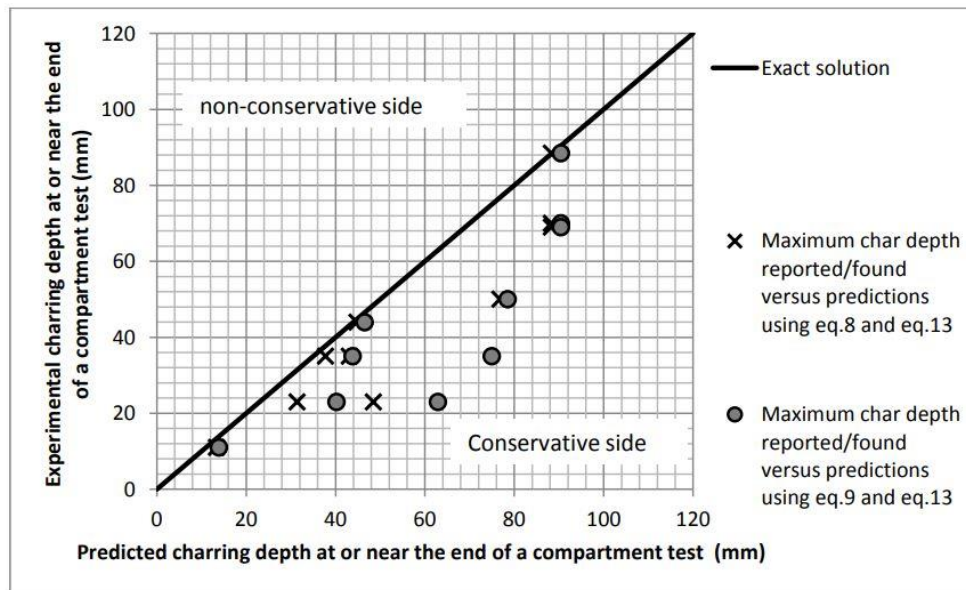


**Figure 3.** Comparison of maximum charring depths from experimental results and calculated predictions (Brandon, 2018b).

### 2.3 Salminen and Hietaniemi (2017)

The study by Salminen and Hietaniemi (2017) discusses the fire design of a 14-story mass timber structure that was an exception to other structures because Finnish regulations only allow buildings of this kind to be limited to only 8 stories. There are two ways to design this type of structure in the case of structural fire design. The first one is the perspective analysis which is based on design the structure using standard fire and design fire classes mentioned in the regulations. The second method is to conduct a performance-based analysis by using fire scenarios that are likely to happen in case of fire. Since the first method was not applicable due to fire regulations, the second method was adopted for the fire design of this structure.

Considering the features of the mentioned building, the first floor was constructed using concrete elements while all the other floors including load bearing elements and elevator shafts were constructed using CLT and LVL. The fire design in the case of this building was based on quantitative risk analysis. Most parts of the building were protected using gypsum boards with 25% surfaces exposed due to regulatory restrictions. The basic idea of the risk analysis is illustrated in the figure below. The second scenario concerns this literature study.

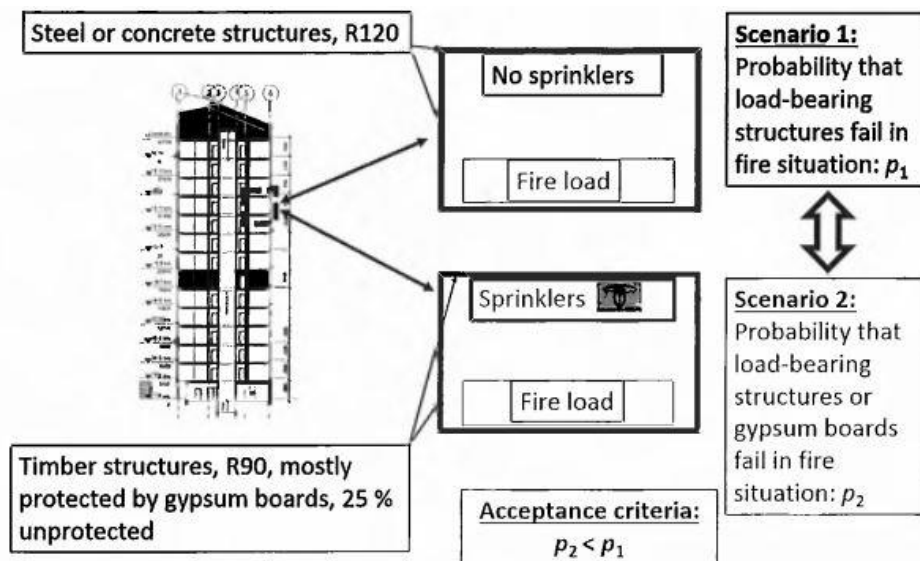


**Figure 4.** Basic idea of quantitative risk analysis for fire design (Salminen & Hietaniemi, 2017).

For calculating the fire temperatures, a model developed by Harmathy (1972a, 1972b) is used. Harmathy (1972a, 1972b) utilized a thermodynamic fire model which gave the fire temperature as a function of time which was influenced by many factors including dimensions of the

compartment, ventilation conditions and enclosure characteristics. From this calculation method, the initial fire load that was calculated was  $420 \text{ MJ/m}^2$  (Salminen and Hietaniemi, 2017). In the initial fire load calculations, the roles of sprinklers, fire brigade and char layer were not considered.

The calculation of char depth using Eurocode 1 and Eurocode 5 was not possible in the fire scenarios used in the performance-based approach, as the methods and formulas can only be applied in standard fire conditions. For this purpose, a modified conductivity model proposed by Hopkin (2011) was used for specific heat capacity and conductivity to satisfy the conditions of Eurocode 5 Annex B. Salminen and Hietaniemi (2017) proposed a simpler modification by multiplying the thermal conductivity by 1.45 to get more reliable results compared to the fire tests that were not conducted using standard fire exposure. The char layer depth analysis was performed in SAFIR software with design analysis assumption based on Eurocode 5.

In the study by Salminen and Hietaniemi (2017), to calculate the fire load  $q$ , an iterative model was used which calculated the fire load first based on the risk analysis and then subsequently calculating the fire temperatures and char depth, then adding more fire load and repeating the iterations until the following criteria is fulfilled (Salminen & Hietaniemi, 2017):

$$q_{i+1} - q_i < 1\% \quad (10)$$

Meaning that the fire load is correct if the difference between two consecutive iterations is less than 1%. As mentioned in the literature, if there is too much exposed timber, the iteration model may not be valid. Considering a 25% exposed timber in this structure, the final calculated fire load was  $820 \text{ MJ/m}^2$  (Salminen and Hietaniemi, 2017). This design method is valid only if the protected surfaces do not contribute to the fire load. Therefore, adequate thickness of gypsum boards is needed. The design provided a standard fire of about 60 minutes (Salminen and Hietaniemi, 2017).

The results from this method were compared with the compartment fire test conducted in Canada by Hevia (2014) due to similarity in the testing conditions with fire load and some parts of unexposed timber. The method accurately predicted the char depth and gave conservative values. The tests provided the charring rate of  $0.95 \text{ mm/min}$  while this method provided a charring rate of  $1.3 \text{ mm/min}$  (Salminen & Hietaniemi, 2017). Therefore, the method can be applied for partially exposed timber buildings.

## 2.4 FprEN 1995-1-2:2023

The next generation of Eurocode 5 will provide detailed guidelines for the structural fire design of timber in standard fire and parametric fire conditions. For the sake of this research, the design parameters for the parametric fire conditions are considered because fuel load and ventilation influences are not considered in the standard fire conditions. As the exposed timber will contribute toward increasing the fuel load, it is essential to consider the parametric fire conditions for research purposes.

Annex A of FprEN 1995-1-2:2023 will provide guidelines for determining the contribution of exposed timber to fire load. For the calculation of charring rate  $\beta_{par}$  in case of unprotected timber, the following equation is given (FprEN 1995-1-2:2023, Equation A.9):

$$\beta_{par} = \beta_n \Gamma^{0.25} \quad (11)$$

Where  $\beta_n$  is the nominal charring rate calculated from FprEN 1995-1-2:2023, equation 5.2 and  $\Gamma$  is the heat factor calculated from EN-1991-1-2:2024, equation A.2.

The formula for design charring depth  $d_{char,t}$  is given as follows (FprEN 1995-1-2:2023, Equation A.10):

$$d_{char,t} = 2 \beta_{par} t_0 \quad (12)$$

Where  $t_0$  is the time at which the charring rate is assumed to be constant and can be calculated using the following equation (FprEN 1995-1-2:2023, Equation A.11):

$$t_0 = 0.009 \frac{q_{d,tot,t}}{o} \quad (13)$$

The design total fire load  $q_{d,tot,t}$  is calculated by using the following equation (FprEN 1995-1-2:2023, Equation A.12):

$$q_{d,tot,t} = q_{d,fi,t} + q_{d,st,t} \quad (14)$$

Where  $q_{d,fi,t}$  is the design value of the fire load density related to the surface area of the compartment and can be determined by using Table E.5, EN 1991-1-2:2024 or by using the values used in the other research literature. For this study, the value was taken from (Buchanan & Östman, 2022).

$q_{d,st,t}$  is the structural fire load density that represents the contribution of exposed CLT or mass timber elements to the fire load in the compartment and can be determined by using the following equation (FprEN 1995-1-2:2023, Equation A.13):

$$q_{d,st,t} = 60 m s_{10} d_{char,t} \alpha_{st} \frac{A_{st}}{A_t} \quad (15)$$

In the above equation (15):

$m$  is the combustion factor from EN 1991-1-2:2024 taken as 0.8.

$s_{10}$  is the rate of heat release of exposed timber members per unit area related to charring rate and having a value of  $0.12 \text{ MW}/\text{m}^2$  per  $\text{mm}/\text{min}$ .

$\alpha_{st}$  is the time dependent modification factor taken as 1.

$A_{st}$  is the area of the exposed CLT or mass timber structural members that are burning inside the compartment and can be calculated from compartment dimensions.

$A_t$  is the total surface area of the compartment.

The methodology of determining the fire load  $q_{d,tot,t}$  due to exposed mass timber or CLT in the compartment is similar to the calculation method of Brandon (2018a, 2018b) where the charr depth  $d_{char,t}$  of the first iteration is used to calculate the structural fire load density  $q_{d,st,t}$  for second iteration. This process is repeated until the difference in charr depth between subsequent iterations becomes less than  $0.5 \text{ mm}$ . When using equation (14) in iterations, the structural fire load density  $q_{d,st,t}$  for the first iteration is taken as zero.

When the criteria for stopping iterations have been achieved, the maximum fire temperature  $\theta_{max}$  can be calculated using the following equation (EN 1991-1-2:2024, Equation A.1):

$$\theta_g = 20 + 1325(1 - 0.324e^{-0.2t*\Gamma} - 0.204e^{-1.7t*\Gamma} - 0.472e^{-19t*\Gamma}) \quad (16)$$

The duration of the heating phase  $t_{max}$  for maximum fire temperature can be calculated using the following equation (EN 1991-1-2:2024, Equation A.9):

$$t_{max} = \max \left[ \left( 0.2 * 10^{-3} \frac{q_{d,t}}{\rho} \right); t_{lim} \right] \quad (17)$$

## 2.5 Xing et al. (2024)

The research by Xing et al. (2024) follows the same pattern of predicting the contribution of exposed timber to the fire load, which is overlooked by many other calculation methodologies. Other concerns discussed in this literature come from the use of parametric fire curves being valid only in the case of non-combustible compartments. In the case of combustible ones, the assumption that 70% of the fuel in the compartment is burned outside is an unjustified assumption with no theoretical basis behind it. Similarly, another point is raised where the use of Eurocode 5 to calculate the charring rates is not accurate due to the non-consideration of increased fire load. This leads to stark differences between experimental and calculated parametric fire curves.

In the research by Xing et al. (2024), a three-stage parametric curve is presented that consists of an ascending phase, a rapid descending stage and a slow cooling phase. Sensitivity analysis is done considering the following parameters, ventilation height, width, exposed area and fire load to determine which parameter is influential in case of fire development. The analysis of various test results from different researchers in Xing et al. (2024) showed that the charring rate increases with the exposed timber surface initially and then becomes relatively constant as the fire develops. This is explained by the following equation (Xing et al., 2024, Equation 1):

$$\beta_{exp} = 29.66 - 47.51 \times 0.93^{exp} \quad (18)$$

In equation (18),  $\beta_{exp}$  is the rate of increase in the charring rate and  $exp$  is the percentage of exposed CLT or exposed structural timber surface in the compartment. Based on the above equation (18), a modified equation for charring rate for a parametric fire curve considering the contribution of exposed timber is presented (Xing et al., 2024, Equation 2):

$$\beta_{par} = 1.5 \beta_0 \frac{0.2 \sqrt{\Gamma} - 0.04}{0.16 \sqrt{\Gamma} + 0.08} \times (1 + 0.01 \beta_{exp}) \quad (19)$$

In equation (19),  $\beta_0$  is one dimensional design charring rate and  $\Gamma$  is the heat rate factor. The values obtained using equation (19) present an error of 13.25%, which is within the accuracy requirements mentioned in Xing et al. (2024). For determining the gas temperature  $T_g$ , following expression is used (Xing et al., 2024, Equation 15):

$$T_g = 6000 \frac{(1 - e^{-0.1\Omega})}{\sqrt{\Omega}} \quad (20)$$

In equation (20), the value  $\Omega$  can be calculated using the following equation (Xing et al., 2024, Equation 16).

$$\Omega = \frac{(A_T - A_0)}{A_0 \sqrt{H_0}} \quad (21)$$

In equation (21),  $A_T$  is the total surface area of the compartment,  $A_0$  is the area of the openings in the compartment and  $H_0$  is the height of the openings. Equation (20) is only applicable in the condition when the percentage of fuel burning outside the compartment is less than 65%. The fuel load  $q_{td}$  can be determined using the following equation (Xing et al., 2024, Equation 26):

$$q_{td} = q_{mfl} + \frac{A_{CLT} \alpha_1 (d_{char} - \eta \beta_{par} t_{max})}{A_T} \quad (22)$$

Equation (22) is similar to the equation (7) used in the method by Brandon (2018a, 2018b). The gas temperature  $T_g$  calculated from equation (20) is compared with the heating stage gas temperature  $\Theta$  calculated according to equation (16), mentioned in FprEN 1995-1-2:2023. Then the following convergence criteria is needed to be satisfied (Xing et al., 2024, Equation 27):

$$\frac{T_g - \Theta}{\Theta} \leq 10\% \quad (23)$$

If this criterion is not fulfilled, the following equation is used for calculating the maximum temperature, and the calculation process is repeated until the final convergence (Xing et al., 2024, Equation 28):

$$\Theta_g = \frac{T_g + \Theta}{2} \quad (24)$$

The parameters that have the most influence on three-stage parametric fire curve are presented in the following order:

Fire Load > Height of the Vent > Width of the Vent > Wood Exposed Area.

Xing et al. (2024) is based exclusively on the fire tests performed on CLT. Therefore, the applicability of this method in the case of solid timber or other timber products may provide varying results.

## 2.6 Summary

In this section, a summary is provided about the observations made during the review process of the five calculation methods, and based on these observations, the differences between the methods are analyzed. The analysis results are reported in Table 1 below. Later in Chapter 3, the usability and results of the methods will be further analyzed using a case study and calculations.

**Table 1.** Comparison of different calculation methods.

<b>Criteria</b>	<b>Brandon, (2016)</b>	<b>Brandon, (2018a, 2018b)</b>	<b>Salminen &amp; Hietaniemi, (2017)</b>	<b>FprEN 1995-1-2:2023</b>	<b>Xing et al. (2024)</b>
<b>Design Approach</b>	Uses one-zone model and combustion model for the determination of fire temperature.	Utilizes an iterative method to determine the charring depth and fire load.	Utilizes a thermodynamic model for the determination of fire temperature inside the compartment.	Utilizes parametric fire curve to determine fire temperature, charring depth and fire load.	Three stage fire curve model, that modifies FprEN 1995-1-2:2023, to account for exposed CLT.
<b>Differences</b>	Focused on the HRR of CLT that is calculated iteratively, to determine the fire temperature.	Utilizes numerical iterations for fire load calculations but accounts for area of the exposed surfaces separately.	Utilizes the thermodynamic model of Harmathy (1972a, 1972b) to determine the heat flux which then gives the fire temperature.	Similar to Brandon (2018a, 2018b), but the area of exposed surfaces is accounted in the structural fire load density.	Accounts for the exposed surfaces directly in the determination of charring rate. Catered exclusively for exposed CLT.
<b>Assumptions</b>	All delamination in exposed CLT happens at the same time.	No second flashover will occur during the burning of fire.	Only 25% of unprotected surfaces can be utilized in the compartment.	No forced draught for calculating fire load and fire temperature.	Fuel load burning outside the compartment is less than 65%.
<b>Limitations</b>	Overestimation of HRR after flashover point and delamination.	No explicit consideration for delamination and second flashover.	Only applicable if the protected surfaces do not contribute to the fire load.	Conservative approach for fire design that may overestimate certain output parameters.	Exclusive to CLT only, not applicable for solid timber and other timber products.
<b>Applicability</b>	Applicable to compartment area upto 100 meter square.	Applicable for large scale mass timber construction.	Applicable to high rise timber buildings with limited exposed surfaces.	A standard guide for fire design in different fire scenarios.	Applicable for CLT buildings with numerous exposed surfaces.

## 3. CALCULATIONS AND RESULTS

### 3.1 Compartment Details

Before discussing the calculations and the results obtained from different calculation methods, it is necessary to describe the compartment details that were used to perform the calculations. The plan of the compartment is given in Figure 5 below:

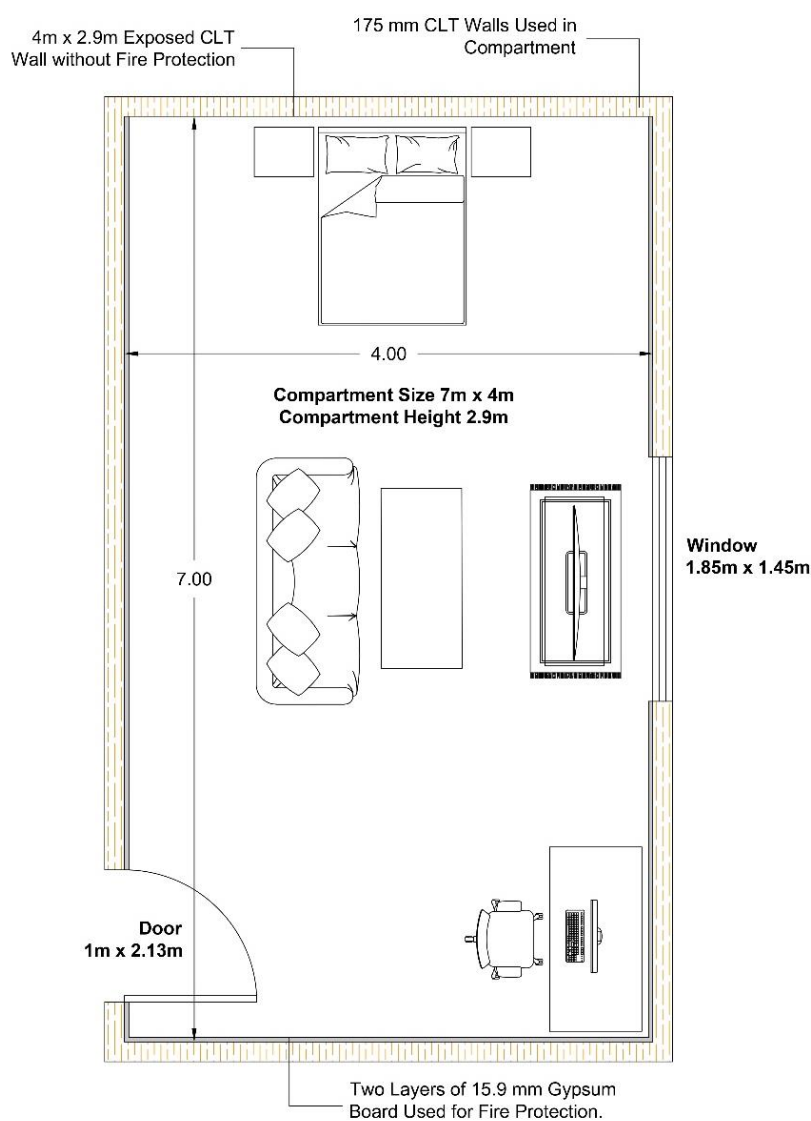


**Figure 5.** Compartment plan used to perform calculations for different methods.

The details of the compartment plan in Figure 5 are as follows:

- The floor area of the compartment is 7 m x 4 m.
- The height of the compartment is 2.9 m.
- The size of the window is 1.85 m x 1.45 m (width x height).
- The size of the door is 1 m x 2.13 m
- A 175 mm thick CLT layer is utilized on all four walls of the compartment.
- One wall, 4 m wide and 2.9 m high, is left exposed while all the other walls are protected using 2 layers of 15.9 mm gypsum board to protect these walls from fire inside the compartment.
- The compartment consists of typical furniture that will contribute as a moveable fire load inside the compartment and this value will be utilized in the calculations further.

### **3.2 Calculation Methodology**

The calculation methodology explains how numerical calculations were performed. For this thesis, there were five methods that were used to calculate certain desired parameters. The calculation methods that were used are listed below:

- Brandon (2016)
- FprEN 1995-1-2:2023
- Brandon (2018a, 2018b)
- Xing et al. (2024)
- Salminen and Hietaniemi (2017)

The desired output parameters that were focused upon while performing calculations using these methods are as follows:

- Maximum fire temperature
- Duration of heating phase for maximum fire temperature
- Charring rate
- Charring depth
- Maximum fire load

All the above-mentioned calculations use different approaches to calculate these parameters. Some methods use simulation models and repetitive iterations to obtain the results, while other

methods utilize formulas from literature based on experimental results obtained from fire tests that emulate natural fire conditions.

The calculation methodology was based on using the above-mentioned methods to perform calculations manually and then conducting a comparative analysis of the obtained results. The software that was used to facilitate performing these calculations is Mathcad Prime version 10.0.1.0.

The details of the calculation methods are already explained in the previous chapter. This chapter will specify the process used to perform calculations, input parameters used in the calculations and the output parameters obtained after performing the calculation. The details of the calculations can be obtained from the Annexes that will be compiled at the end of this thesis, for all calculation methods.

### 3.3 Brandon (2016)

Brandon (2016) method is an iterative method that utilizes SP-Timfire which is a two-zone model to calculate different parameters. The most important parameters for this method are heat release rate of CLT and the moveable fire load that is based on the area of exposed CLT inside the compartment. Both parameters increase as the fire progresses until the maximum fire temperature is obtained in the growth phase of the fire.

While performing the calculations, one setback was observed. There is a parameter that needs to be determined for calculating the fire temperature, namely the rate of heat loss through compartment boundaries  $Q_w$ . To calculate this parameter, the following equation is used (EN 1991-1-2:2002, Equation D.5):

$$Q_w = (A_t - A_{h,v}) h_{net} \quad (25)$$

Where  $A_t$  is the total surface area of the compartment,  $A_{h,v}$  is the area of ventilation opening and  $h_{net}$  is the net heat flux.

To calculate  $h_{net}$  the following equation is used (EN 1991-1-2:2002, Equation 3.1):

$$h_{net} = h_{net;c} + h_{net;r} \quad (26)$$

Where  $h_{net;c}$  is the convective heat flux calculated using EN 1991-1-2:2002, Equation 3.2 and  $h_{net;r}$  is the radiative heat flux calculated using EN 1991-1-2:2002, Equation 3.3.

$$h_{net;c} = \alpha_c (\theta_g - \theta_m) \quad (27)$$

$$h_{net;r} = \phi \cdot \varepsilon_m \cdot \varepsilon_f \cdot \sigma \cdot [(\theta_r + 273)^4 - (\theta_m + 273)^4] \quad (28)$$

In the above equations (27) and (28),  $\theta_g$  is the gas temperature in the vicinity of fire exposed member,  $\theta_m$  is the surface temperature of the member and  $\theta_r$  is the effective radiation temperature of the fire environment.

Determining these temperatures is not possible without the use of simulation software to obtain the actual and precise values needed for calculations, as described by Brandon (2016). As the scope of this research is based on performing calculations using Mathcad, the use of simulation software is outside the scope. Therefore, Brandon's (2016) method was neglected for the purpose of performing calculations in this research.

### 3.4 FprEN 1995-1-2:2023

FprEN 1995-1-2:2023 provides equations for parametric fires to calculate different parameters. The second-generation Eurocode provides additional equations for calculating the compartment temperature  $T_g$  and the charring depth  $d_{char,t}$  of unprotected members, which takes into consideration the exposed surfaces inside the compartment. FprEN 1995-1-2:2023 also suggests performing iterations in the sense that the fire load density  $q_{d,fi,t}$  is selected at the beginning to perform the calculations in the first iteration. In the second iteration, the structural fire load density  $q_{d,st,t}$  is calculated and added to the previous one to obtain the total fuel load density  $q_{d,tot,t}$  for the next iteration. In these calculations, the main goal is to find the contribution of exposed timber surfaces. Therefore, the structural fire load  $q_{d,st,t}$  is the main component representing exposed timber in the form of combusting surface area,  $A_{st}$ .

Brandon (2018a, 2018b) has concluded that approximately 70% of the contribution of the timber combusts outside the fire compartment, for at least the duration of the fully developed phase of a similar compartment without combustible linings. In this research, the fire load burning outside the compartment is estimated by using the effective charring model introduced in figure A.1 of EN 1995-1-2:2004. The principle of the model is illustrated in Figure 6 below.

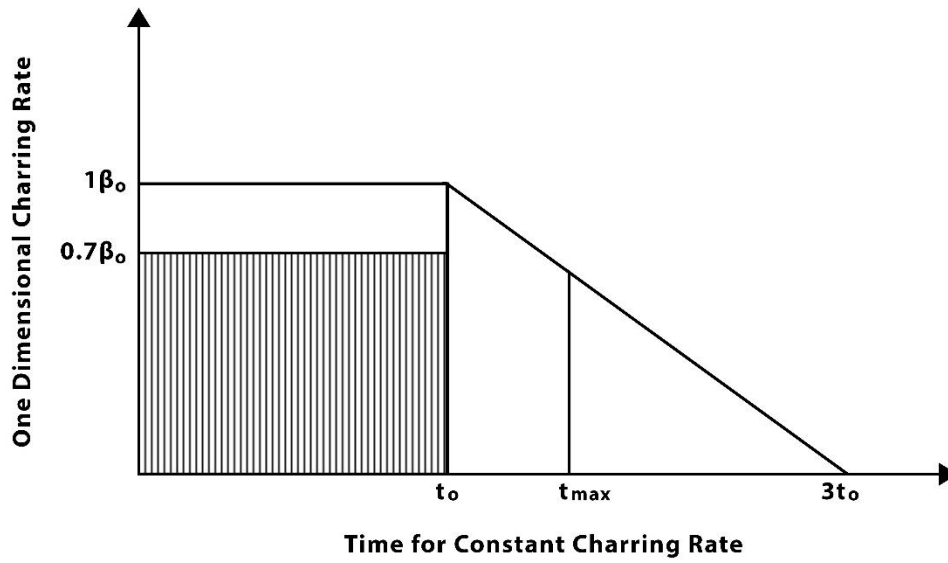


**Figure 6.** Comparison between  $t_o$  and  $\beta_o$ .

In the effective charring model and Figure 6, parameter  $t_o$  is the time period with a constant charring rate. The charring rate is assumed to be constant for the entire heating phase, i.e. the fully developed phase. In this research, it is assumed that 70% of the area, defined by  $t_o$  and  $\beta_o$ , is the proportion of the structural fire load that burns outside the compartment. The proportion of the structural fire load burning inside can now be calculated as the ratio between the unshaded area and the total area defined by  $\beta_o$ ,  $t_o$  and  $3t_o$ . The unshaded area, representing the proportion of fire load burning outside the compartment, is calculated using equation (29) mentioned below:

$$\text{Remaining Area} = 0.3 * \beta_o * t_o + \frac{1}{2} * 2t_o * \beta_o = 1.3 * \beta_o * t_o \quad (29)$$

The percentage of the remaining area of fire load in the graph can be calculated using equation (30) mentioned below:

$$\% \text{ of Remaining Area} = \frac{1.3 * \beta_o * t_o}{(\beta_o * t_o) + \frac{1}{2} * 2t_o * \beta_o} = 0.65 \quad (30)$$

Equation (14) for the design total fire load  $q_{d,tot,t}$ , can now be modified to address the reduction:

$$q_{d,tot,t} = q_{d,fi,t} + 0.65 q_{d,st,t} \quad (31)$$

The details of the calculations can be found in Annex A at the end of this thesis. Table 2 below describes the input parameters and related equations that were used for performing calculations

for FprEN 1995-1-2:2023 method. The output parameters obtained after performing calculations are mentioned in Table 3 below.

**Table 2.** Input parameters and related equations in the FprEN 1995-1-2:2023 method

Parameter	Value	Unit	Description	Reference
$q_{d;fi,t}$	550	$\frac{MJ}{m^2}$	Fire Load Density	Buchanan & Östman, (2022)
$\beta_0$	0.65	$\frac{mm}{min}$	One Dimensional Charring Rate	FprEN 1995-1-2:2023, Table 5.4
$\beta_n$	0.707	$\frac{mm}{min}$	Nominal Charring Rate	FprEN 1995-1-2:2023, Equation 5.2
$\rho$	470	$\frac{kg}{m^3}$	Density of Spruce	Assumed for CLT
$c$	1530	$\frac{J}{kg K}$	Specific Heat Capacity at 20 °C	FprEN 1995-1-2:2023, Table 8.1
$\lambda$	0.12	$\frac{W}{m K}$	Thermal Conductivity at 20 °C	FprEN 1995-1-2:2023, Table 8.1
$A_v$	2.683	$m^2$	Ventilation Area	Calculated from Compartment Plan
$A_t$	119.8	$m^2$	Total Surface Area of Compartment	Calculated from Compartment Plan
$h_v$	1.45	$m$	Opening height	Compartment Plan
$O$	0.028	$m^{1/2}$	Opening Factor	EN 1991-1-2:2024, Equation A.2
$\beta_{par}$	0.826	$\frac{mm}{min}$	Parametric Charring Rate	FprEN 1995-1-2:2023, Equation A.9
$A_f$	28	$m^2$	Floor Area	Calculated from Compartment Plan
$d_{char}$	74.474	$mm$	Design Charring Depth	FprEN 1995-1-2:2023, Equation A.10
$\Gamma$	1.856	-	Heat Rate Factor	EN 1991-1-2:2024, Equation A.2

**Table 3.** Output parameters and related equations in the FprEN 1995-1-2:2023 method

Parameter	Value	Unit	Description	Reference
$\theta_{max}$	1037.636	$^{\circ}C$	Maximum Fire Temperature	EN 1991-1-2:2024, Equation A-1
$t_{max}$	60.12	$min$	Time to achieve maximum fire temperature	EN 1991-1-2:2002, Equation A-9
$\beta_{par}$	0.826	$\frac{mm}{min}$	Parametric Charring Rate	FprEN 1995-1-2:2023, Equation A.9
$d_{char}$	74.474	$mm$	Charr Depth	FprEN 1995-1-2:2023, Equation A.10
$q_{td}$	140.777	$\frac{MJ}{m^2}$	Final Fuel Load Density	FprEN 1995-1-2:2023, Equation A.12

### 3.5 Brandon (2018a, 2018b)

Brandon (2018a, 2018b) method is also an iterative method that utilizes a fire model that takes into consideration the area of exposed CLT in the calculations. The main parameters that are changing in every iteration are the fuel load  $q_{td}$ , and the charring depth  $d_{char;end}^i$ . The maximum fire temperature in a compartment can be determined through iterative calculation. The conditions for stopping the iterations are described in Brandon (2018a, 2018b) as follows:

- The charring depth converges which means that the difference between charring depths in consecutive iterations come out to be 0.1%.
- The maximum time, which refers to the time needed to achieve the maximum fire temperature in the fully developed phase, becomes continuous, which means that we have a continuously developing phase because the maximum time keeps on increasing after every iteration.

The details of the calculations can be found in Annex B at the end of this thesis. Table 4 below describes the input parameters and related equations that were used for performing calculations for Brandon (2018a, 2018b) method. The output parameters obtained after performing calculations are described in Table 5 below:

**Table 4.** Input parameters and related equations in the Brandon (2018a, 2018b) method

Parameter	Value	Unit	Description	Reference
$q_{mfl}$	550	$\frac{MJ}{m^2}$	Moveable Fire Load Density	Buchanan & Östman, (2022)
$A_{CLT}$	11.6	$m^2$	Area of Exposed CLT	Calculated From Compartment Plan
$\alpha_1$	5.39	$\frac{MJ}{m^2 * mm}$	Correction Factor	Buchanan & Östman, (2022)
$\beta_n$	0.707	$\frac{mm}{min}$	Nominal Charring Rate	FprEN 1995-1-2:2023, Equation 5.2
$\rho$	470	$\frac{kg}{m^3}$	Density of Spruce	Assumed for CLT
$c$	1530	$\frac{J}{kg K}$	Specific Heat Capacity at 20 °C	FprEN 1995-1-2:2023, Table 8.1
$\lambda$	0.12	$\frac{W}{m K}$	Thermal Conductivity at 20 °C	FprEN 1995-1-2:2023, Table 8.1
$A_v$	2.683	$m^2$	Ventilation Area	Calculated from Compartment Plan
$A_t$	119.8	$m^2$	Total Surface Area of Compartment	Calculated from Compartment Plan
$h_v$	1.45	$m$	Opening height	Compartment Plan
$O$	0.027	$m^{1/2}$	Opening Factor	Brandon (2018a), Equation 3
$\beta_{par}$	0.826	$\frac{mm}{min}$	Parametric Charring Rate	Brandon (2018a), Equation 8
$A_f$	28	$m^2$	Floor Area	Calculated from Compartment Plan
$t_{max}$	0.954	$h$	Maximum Time for Fire Development	Brandon (2018a), Equation 4

**Table 5.** Output parameters and related equations in the Brandon (2018a, 2018b) method

Parameter	Value	Unit	Description	Reference
$T_{f;max}$	1058.807	$^{\circ}C$	Maximum Fire Temperature	EN-1991-1-2-2024, Equation A-1
$q_{td}$	156.232	$\frac{MJ}{m^2}$	Final Fuel Load Density	Brandon (2018b), Equation 16
$t_{max}$	69.54	$min$	Time to achieve maximum fire temperature	Brandon (2018a), Equation 4
$\beta_{par}$	0.826	$\frac{mm}{min}$	Parametric Charring Rate	Brandon (2018a), Equation 8
$d_{char}$	86.109	$mm$	Charr Depth	Brandon (2018a), Equation 12

### 3.6 Xing et al. (2024)

The method by Xing et al. (2024) also involves predicting the contribution of exposed timber in fire load. In this method, an additional formula is presented for charring rate  $\beta_{exp}$  which considers the exposed timber area in the compartment and the value of this parameter varies with the exposed percentage of timber surface inside the compartment. The literature also provides an additional formula for parametric charring rate  $\beta_{par}$ . It also provides a different formula for maximum gas temperature  $T_g$  which has a separate convergence criterion to be satisfied by performing consecutive iterations.

In short, this method further develops the formulas of parametric fires and makes them more applicable in cases where the amount of exposed timber surfaces inside the compartment varies. The formulas and detailed calculations are provided in Annex C at the end. Table 6 below provides the details of input parameters and related equations used to perform calculations for Xing et al. (2024) method. The output parameters obtained after using these input parameters to perform the calculations are mentioned in Table 7 below.

**Table 6.** Input parameters and related equations in the Xing et al. (2024) method

Parameter	Value	Unit	Description	Reference
$q_{td}$	156.232	$\frac{MJ}{m^2}$	Fire Load Density	Calculated in Brandon (2018a, 2018b)
$\beta_0$	0.65	$\frac{mm}{min}$	Basic Charring Rate	FprEN 1995-1-2:2023, Table 5.4
$exp$	10	-	Exposure Value	Assumed
$\beta_{exp}$	6.666	-	Rate of increase in charring rate corresponding to exposed surfaces	Xing et al. (2024), Equation 1
$\Gamma$	1.856	-	Heat Rate Factor	Calculated in Brandon (2018a, 2018b)
$A_w$	2.683	$m^2$	Area of Windows	Calculated from Compartment Plan
$A_t$	119.8	$m^2$	Total Surface Area of Compartment	Calculated from Compartment Plan
$\Omega$	35.641	-	Constant Value	Xing et al. (2024), Equation 16

**Table 7.** Output parameters and related equations in the Xing et al. (2024) method

Parameter	Value	Unit	Description	Reference
$T_g$	976.556	$^{\circ}C$	Maximum Fire Temperature	Xing et al. (2024), Equation 15
$t_{max}$	69.42	$min$	Time to achieve maximum fire temperature	Xing et al. (2024), Equation 23
$\beta_{par}$	0.811	$\frac{mm}{min}$	Parametric Charring Rate	Xing et al. (2024), Equation 2
$d_{char}$	84.507	$mm$	Charr Depth	Xing et al. (2024), Equation 25
$q_{td}$	156.232	$\frac{MJ}{m^2}$	Final Fuel Load Density	Brandon (2018b), Equation 16

### 3.7 Salminen & Hietaniemi (2017)

This method was adopted for the fire design of a fourteen-storey building that was made from mass timber members. The methodology for the design is explained in detail prior in the theoretical background chapter. The main formulas for the calculation of fire temperature are taken from Harmathy (1972a, 1972b). The formulas consisted of calculating the heat flux  $q_E$  and then using it to calculate the gas temperature  $T_g$ . The calculations for charring rate  $\beta_{par}$  and charring depth  $d_{char}$  are done using equations from the FprEN 1995-1-2:2023.

Iterations were performed for calculating the heat flux and fire temperatures, up to the point where the subsequent iterations provide the most accurate values. The details of the formulas and calculations can be found in Annex D at the end of this thesis. Table 8 below provides the details of the input parameters and related equations used in this method. The output parameters obtained from this calculation method are mentioned below in Table 9.

**Table 8.** Input parameters and related equations in the Salminen and Hietaniemi (2017) method

Parameter	Value	Unit	Description	Reference
$A_w$	2.683	$m^2$	Area of Windows	Calculated from Compartment Plan
$A_t$	119.8	$m^2$	Total Surface Area of Compartment	Calculated from Compartment Plan
$A_{fz}$	11.6	$m^2$	Fire Area	Calculated from Compartment Plan
$c_g$	1100	$\frac{J}{kg K}$	Specific Heat of Air	Assumed
$G_o$	954.1	$kg$	Mass of CLT	Harmathy (1972a)
$\rho_a$	1.225	$\frac{kg}{m^3}$	Density of Air	Known Constant
$g$	9.81	$\frac{m}{s^2}$	Acceleration Due to Gravity	Known Constant
$\phi$	9.154	$\frac{kg}{s}$	Ventilation Parameter	Harmathy (1972a), Equation 16

$l$	1.698	$m$	Flame Height	Harmathy (1972a), Equation 38b
$U_a$	2.29	$\frac{kg}{s}$	Flow Rate of Air	Harmathy (1972a), Equation 17
$R$	0.072	$\frac{kg}{s}$	Rate of change of mass of fuel	Harmathy (1972a), Equation 28a
$\beta$	1	-	Constant	Harmathy (1972a)
$Z$	1.05	-	Constant	Harmathy (1972a)
$\eta$	0.9	-	Constant	Harmathy (1972a)
$T_o$	20	$^{\circ}C$	Ambient Temperature	Assumed
$k_c$	0.15	$\frac{J}{m\ s\ K}$	Thermal conductivity of Lining Material	Harmathy (1972b)
$k_d$	$0.12 \cdot 10^{-6}$	$\frac{m^2}{s}$	Thermal Diffusivity of Lining Material	Harmathy (1972b)
$\tau$	12419.75	$sec$	Time of Primary Burning	Harmathy (1972b), Equation 44a
$\sigma$	$5.670 \cdot 10^{-8}$	$\frac{W}{m^2\ K^4}$	Stefan Boltzmann Constant	Known Constant
$\Delta H_c$	$26 \cdot 10^6$	$\frac{J}{kg}$	Heat of Combustion for charr layer	Harmathy (1972b)
$\Delta H_v$	$15 \cdot 10^6$	$\frac{J}{kg}$	Heat of Combustion for volatile gases	Harmathy (1972b)

**Table 9.** Output parameters and related equations in the Salminen and Hietaniemi (2017) method

Parameter	Value	Unit	Description	Reference
$T_g$	1067.754	$^{\circ}C$	Maximum Fire Temperature	Harmathy (1972b), Equation 61
$q_{td}$	82.25	$\frac{kg}{m^2}$	Final Fuel Load Density	Harmathy (1972b)
$t_{max}$	36.42	$min$	Time to achieve maximum fire temperature	EN 1991-1-2:2002, Equation A-9
$\beta_{par}$	1.005	$\frac{mm}{min}$	Parametric Charring Rate	FprEN 1995-1-2:2023, Equation A.9
$d_{char}$	54.874	$mm$	Charr Depth	FprEN 1995-1-2:2023, Equation A.10

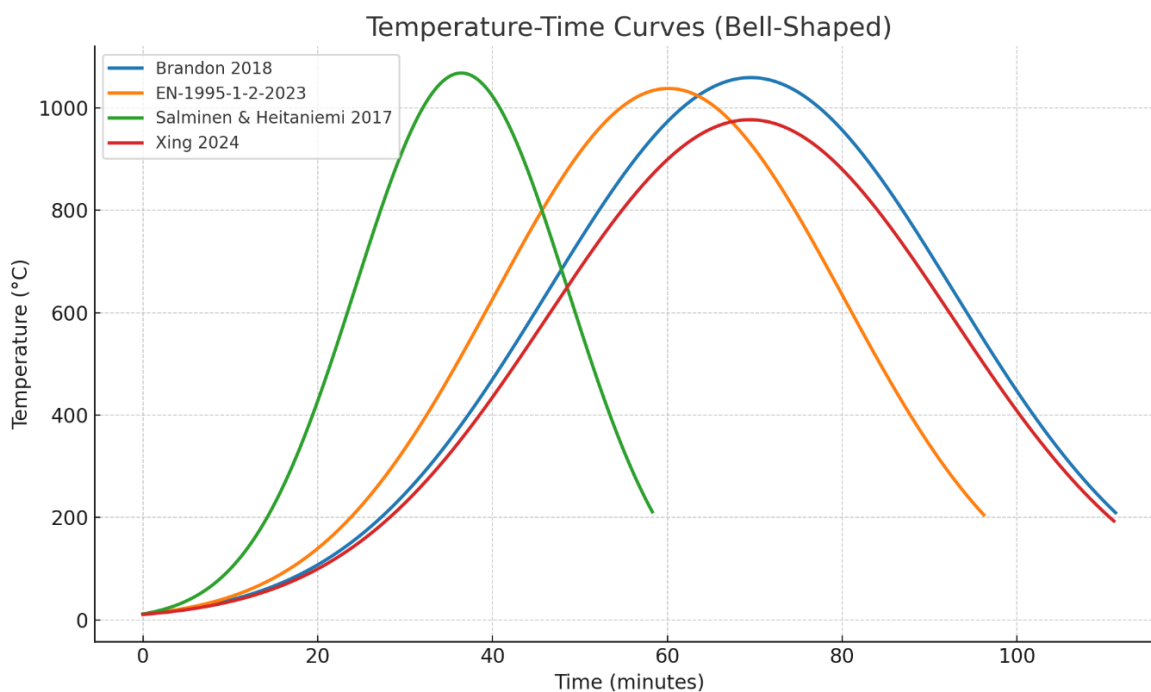
### 3.8 Summary of Results

Table 10 below compiles the output parameters including maximum fire temperature, duration of the heating phase for maximum fire temperature, charring rate, charring depth and fire load, obtained from the four calculation methods.

**Table 10.** Compilation of results from calculation methods

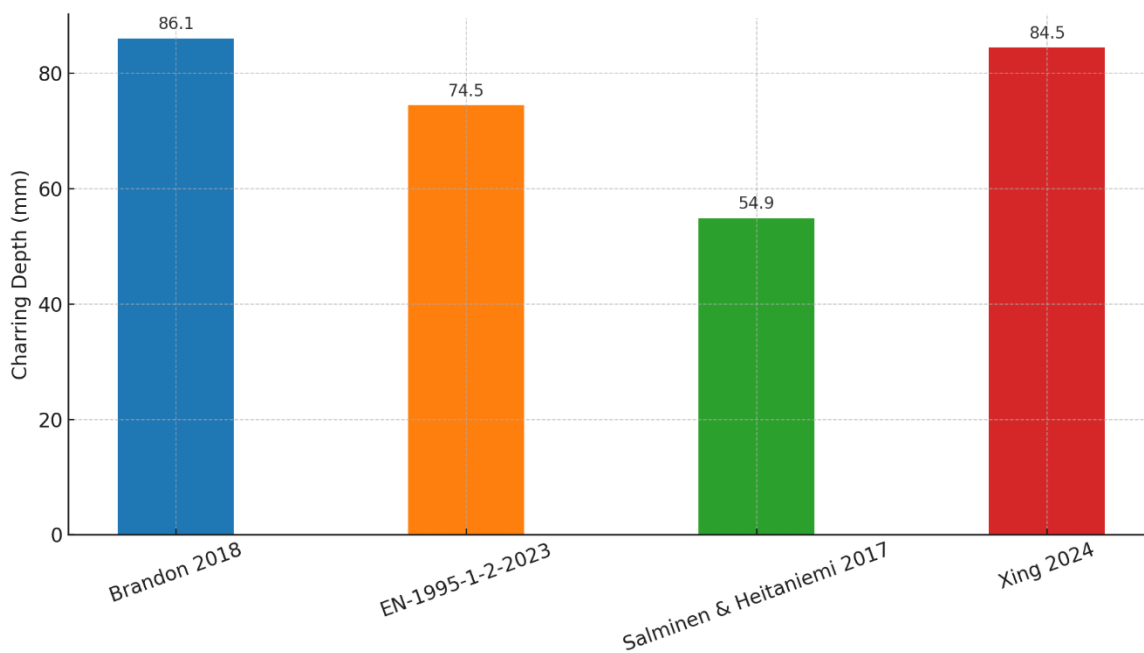
Parameter	FprEN 1995-1-2:2023	Brandon (2018a, 2018b)	Xing et al. (2024)	Salminen and Hietaniemi (2017)
$T_g (^{\circ}C)$	1038	1059	977	1067
$t_{max}(min)$	60.1	69.5	69.4	36.4
$\beta_{par}(\frac{mm}{min})$	0.83	0.83	0.81	1.01
$d_{char}(mm)$	74	86	85	55
$q_{td}(\frac{MJ}{m^2})$	141	156	156	82

Figure 7 provides a visual representation of compartment temperatures over time for all the calculation methods. This image is generated using ChatGPT version 4.0. The peak temperatures and time were taken from Table 10, while the parameters for the temperature and time in the decay phase were defined and calculated by ChatGPT version 4.0 based on the formulas of Eurocode 5 for the decay phase of parametric fires. The shape of the curve was defined in ChatGPT version 4.0 to generate typical inverted bell-shaped curves, common for most parametric fire curves.



**Figure 7.** *Compartment temperature vs. time curve for different calculation methods. (AI Generated)*

In addition, bar graphs are used to compare calculated charring rates and charring depths. Figure 8 provides a comparison of charring depths for all calculation methods. Figure 9 provides a comparison of charring rates for all these calculation methods.



**Figure 8.** Comparison of charring depths determined by different calculation methods.

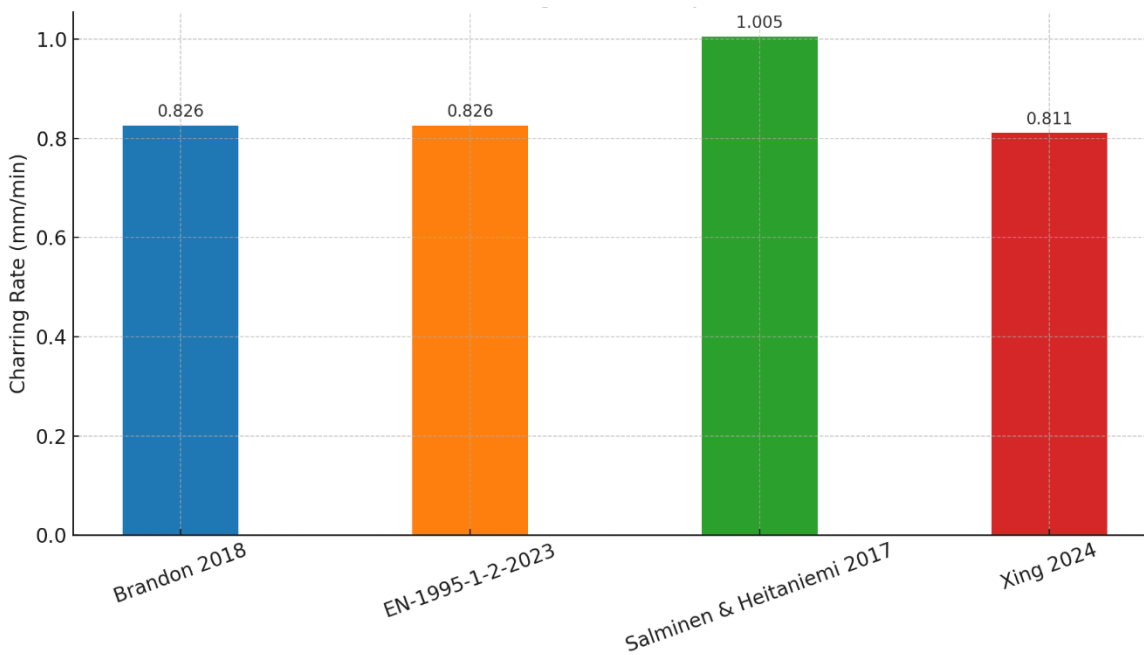


**Figure 9.** Comparison of charring rates determined by different calculation methods

## 4. ANALYSIS AND DISCUSSION

### 4.1 Introduction

Structural fire design for mass timber structures and members utilizing CLT components presents a complicated task of balancing the safety of the structure, precision in the design processes and compliance with the regulations for fire safety design. The analysis compares four key methods discussed previously namely Brandon (2018a, 2018b), FprEN 1995-1-2:2023, Salminen and Hietaniemi (2017) and Xing et al. (2024). This analysis considers the background literature and calculation results from these methods to discuss the following key parameters:

- Differences in input parameters
- Methodological framework
- Reasons for Divergences in Results
- Exposed mass timber vs. CLT
- Area of Exposed Timber vs. Fire Load
- Exposed Timber vs. Decay Phase

### 4.2 Differences in input parameters

When considering the structural fire design of timber structures and specifically in case of performing calculations, the methods are highly sensitive to the input parameters being used. While some of the input parameters remain the same in most of these methods, all four calculation methods utilize unique input parameters that reflect on the design philosophies of these methods. Careful consideration of these input parameters is essential to understand the variability of the output parameters obtained.

#### 4.2.1 FprEN 1995-1-2:2023

As a prescriptive design approach, FprEN 1995-1-2:2023 relies on standardized tables and formulas. The charring rates are specific to the material being used, specifically the nominal charring rate  $\beta_o$  whose value is taken from Table 5.4, FprEN 1995-1-2:2023. The fuel load density  $q_{td}$  can be taken from EN 1991-1-2:2024 using table E.5, or it can be taken from the National

Annexes. In this research, the fuel load density is taken from Buchanan and Östman (2022). In the case of FprEN 1995-1-2:2023, it is assumed that 70% of the structural fire load burns outside the compartment during the fully developed phase. FprEN 1995-1-2:2023 minimizes the need for geometric specifications of the compartment by limiting the calculations to the parameters of the exposed fire area and ventilation parameter in the form of an opening factor  $O$ .

#### **4.2.2 Brandon (2018a, 2018b)**

This design method is a combination of empirical and iterative analysis, where the main driving factors are based on compartment specific temperatures. This is reflected in the moveable fuel load density  $q_{td}$ , which considers the combustible contents of the compartment as well as an addition to the structural elements. The calculated charring rates and opening factors are in line with the results of FprEN 1995-1-2:2023 method. In comparison to FprEN 1995-1-2:2023, the provision of 70% of the fire burning outside the compartment is considered in the iterative formula for fuel load, where the factor  $(0.7 * \beta_{par} * t_{max})$  signifies this phenomenon. This method also introduces the constant  $\alpha_1$  which is a correction factor for the boundary conditions of the compartment.

#### **4.2.3 Xing et al. (2024)**

One specific distinction of this method regarding input parameters is that it takes the fuel load density directly from Brandon (2018a, 2018b) method. While some of the parameters for this method are also derived from FprEN 1995-1-2:2023, what makes Xing et al. (2024) different is the specific focus on modifying the formulas from FprEN-1995-1-2:2023 to account for the role of exposed timber in calculations. This is indicated by the factor  $\beta_{exp}$ , which represents the percentage increase in the charring rate related to the exposed surface and then provides a modified equation for the calculation of parametric charring rate.

#### **4.2.4 Salminen and Hietaniemi (2017)**

The design approach for this method is based on a combination of Eurocode 5 and Harmathy (1972) Part 1 and Part 2 for heat flux modelling. This method specifically considers the thermodynamic characteristics of the compartment, which is why the input parameters are unique and different from other calculation methodologies discussed previously. The ventilation

parameters  $\phi$ , directly considers the airflow in the compartment and flame development. The heat flux calculations utilize the radiative exchange in the compartment boundaries which comes with unique input parameters like flame height  $l$ , flow rate of the air entering from the lower third of the compartment opening  $U_a$  and the rate of change of fuel mass  $R$ . Material properties like the density and specific heat of the air are input parameters unique for this method.

### 4.3 Methodological Framework

The core methodology behind each fire design method is essential when discussing the predictive behavior of these methods and sensitivity to Input parameters.

#### 4.3.1 FprEN-1995-1-2:2023

This calculation method is based on the parametric fire model, which utilizes equations from Annex A of FprEN 1995-1-2:2023 and EN 1991-1-2:2024 to determine key output parameters such as charring rate, charring depth, fire temperatures and the time taken to achieve the maximum fire temperature.

In the first iteration, the method starts by determining the parametric charring rate  $\beta_{par}$ , then moving towards the calculation of fuel load density, which is calculated or taken from the respective tables of Eurocode 1 and 5. Then the charring depth  $d_{char}$ , the time for the fully developed phase of the fire  $t_{max}$  and the maximum fire temperature  $\theta_{max}$  is calculated. In the next iteration, the structural fire load density is calculated and added into the fuel load density, and the charring depth is calculated. These two parameters are consecutively calculated performing iterations until the difference between charring depth converges to a difference of 0.5 mm. Then the iterations can be stopped and the final  $t_{max}$  and  $\theta_{max}$  can be calculated.

#### 4.3.2 Brandon (2018a, 2018b)

Like FprEN 1995-1-2:2023, the fuel load density and charring rate are calculated first. The key difference between these two methods comes from the area of CLT determination  $A_{CLT}$ . In FprEN 1995-1-2:2023, the first iteration does not take the exposed surfaces into account. In the second iteration, the exposed surfaces are considered in the fire load, in the form of  $\alpha_{st}$ . While in Brandon (2018a, 2018b) method, the area of CLT is calculated and considered in the very first iteration for determining the fuel load density  $q_{td}$ . Then the iterations are performed in a similar way to FprEN

1995-1-2:2023 for determining charring depth and fuel load density, until the charring depths in consecutive iterations converge to a point of 0.1% difference.

### 4.3.3 Xing et al. (2024)

For this method, the fuel load density  $q_{td}$  is directly taken from Brandon (2018a, 2018b). The parametric charring rate is calculated by using equation (19), considering the exposure factor  $\beta_{exp}$ . In determining the fire temperature, two fire temperatures are calculated. First, a maximum parametric fire temperature  $\theta_{max}$  is calculated using, for example, FprEN 1995-1-2:2023. Then the fire temperature is calculated using equation (20), Xing et al. (2024). This method provides convergence criteria for the fire temperature utilizing equation (23). If this criterion is not satisfied, perform further iterations until the convergence is satisfied.

### 4.3.4 Salminen and Hietaniemi (2017)

The calculation methodology by Salminen and Hietaniemi (2017) is very different from the other methods when it comes to the determination of fire temperature. In this method, the exposed surfaces are regarded as the weight of the CLT or exposed mass timber, unlike other methods that consider the area of exposed surfaces. The method specific parameters also include the ventilation parameter  $\phi$ , flame height  $l$ , flow rate of air  $U_a$ , and rate of change of fuel mass  $R$ .

The calculation of fire temperature is a process where at first, a fire temperature is assumed, and then effective heat flux  $q_E$  and the fire temperature  $T_g$  are calculated (Harmathy, 1972b, Equations 51 and 61). Iterations are performed consecutively till the difference between the assumed and actual fire temperatures becomes considerably negligible. There are no specific criteria for convergence in this method.

Another difference in this method is that for determining the fuel load density. The mass of CLT or exposed mass timber is divided by the area of the exposed surface to get the fuel load density. The equations from FprEN 1995-1-2:2023 can be used to determine the charring depth  $d_{char}$  and time for maximum fire temperature  $t_{max}$ .

## 4.4 Reasons for Divergences in Results

Despite being applied to the same compartment geometry and timber material, the four methods produce varying output parameters for fuel load, charring rate, charring depth, maximum fire temperature and time for maximum fire temperature. These differences not only arise from the input parameters, but the differences in the design principles that each of these methods utilize to produce the output parameters.

A potential reason behind the divergence of output parameters in these methods is the intended use of these calculation methods. This can be accessed based on compliance, simulation and engineering flexibility.

FprEN 1995-1-2:2023 is designed for regulatory compliance and ease of application when it comes to structural fire design. It provides a conservative approach to account for variable unknowns during the progression of fire in the compartment. The basis for the results is not to be matched with the experimental results, but rather to provide a safe upper limit for the structural fire design.

Brandon (2018a, 2018b) method is utilized when engineering flexibility is desirable. The goal is to provide some degree of realism in structural fire design practices without relying heavily on deep simulation models. It modifies the Eurocode equations by introducing iterative modifiers to account for surface protection, fuel load change and convergence behavior. Therefore, producing output parameters that are more in line with custom simulations rather than code compliance.

Xing et al. (2024) method is an amalgamation of theoretical fire dynamics and simplified engineering use. It provides modifiers for FprEN 1995-1-2:2023 to account for exposed surface contributions. This balance results in output parameters that are less conservative than FprEN 1995-1-2:2023.

Salminen and Hietaniemi (2017) method is intended for realistic simulations when it comes to research or performance-based design. The method is based on rigorous input parameters which yield more accurate and sometimes lower charring depths, particularly in the case of compartments that have lower flashover durations and adequate protection.

## 4.5 Exposed Mass Timber vs. CLT

The calculations performed for the four methods were utilizing CLT as the structural element for walls in the compartment. The main assumption in calculations was that there is no delamination occurring during the progression of the fire. The effect of delamination is a variable that is very tricky to calculate in natural fire experiments and modeling this parameter in design methodology is a far greater and complicated task. Thus, for the purpose of simplification, the delamination is not considered.

To draw a comparison of what changes will occur when it comes to the design approach in case of exposed mass timber and CLT, some of the differences in fire performance in the case of CLT and exposed mass timber are described below:

- **Charring Behavior:** In case of CLT, delamination can lead to char fall-off which will cause reignition for the newly exposed lamella. For exposed mass timber, a more stable char layer is formed which can be predicted more easily.
- **Fire Resistance:** CLT will have lesser fire resistance due to delamination and exposure of new layers of lamella during fire progression while exposed mass timber provides better fire resistance due to robustness and homogenous composition of structural element.
- **Charring Rate:** In the case of CLT, the charring rate has a non-linear progression due to delamination and glue-line failure while for exposed mass timber it is linear and more predictable.
- **Design Complexity:** For CLT, there is a need for simulative modelling for delamination and charr fall-off while for exposed mass timber, simplified design assumptions can be used.
- **Protective Strategies:** The use of CLT in compartments is limited to a certain degree when it comes to the degree of exposure and needs encapsulation. While exposed mass timber elements can be utilized unprotected in certain scenarios.

Considering the above-mentioned parameters, the choice of design methods when it comes to exposed CLT and exposed mass timber can be selected as follows:

- **FprEN 1995-1-2:2023:** Ideal for exposed mass timber and can be used for exposed CLT but lacks the involvement for delamination.

- **Brandon (2018a, 2018b)**: Ideal for exposed mass timber but limited for exposed CLT as higher exposed areas in the compartment leads to convergence criteria not being satisfied.
- **Xing et al. (2024)**: Ideal for both exposed mass timber and exposed CLT as this method accounts for decay modelling which can consider the delamination and the exposure of new CLT lamella in time-based fuel contributions.
- **Salminen and Hietaniemi (2017)**: Ideal for exposed mass timber and good for exposed CLT as well because the thermodynamic modelling of Harmathy (1972a, 1972b) method can handle material transitions during fire progression.

## 4.6 Area of Exposed Timber vs. Fire Load

To understand how the area of exposed mass timber affects the fire load during a fire, calculations were first performed assuming that all four compartment walls are exposed, and then assuming that only one wall is exposed. These calculations were done using the FprEN 1995-1-2:2023 method and the results are reported in Annex A. The calculation results are reported in table 11 below. It provides a comparison of output parameters between 4 walls and one wall of the compartment exposed to fire.

**Table 11.** Comparison of output parameters according to FprEN 1995-1-2:2023 calculations when one wall and four walls are exposed to fire.

Parameter	Unit	4 Walls Exposed	1 Wall Exposed
$\theta_{max}$	$^{\circ}C$	1299	1038
$t_{max}$	$min$	86.9	60.1
$\beta_{par}$	$\frac{mm}{min}$	0.83	0.83
$d_{char}$	$mm$	154	74
$q_{td}$	$\frac{MJ}{m^2}$	203.5	140.8

It is evident from Table 11 that the fire load with four walls exposed is 30% higher compared to the fuel load with only one wall exposed in the compartment. Similarly, other output parameters also increased due to the greater area of exposure in the compartment.

Out of all the output parameters given in Table 11, charring depth  $d_{char}$  is the most concerning. While the fire load is increased 30% when four walls are exposed, the increase in charring depth is almost double. Keeping in mind the structural integrity of the compartment, the thickness of CLT used for the walls of the compartment was 175 mm. A charring depth of 154 mm means that the structural integrity of the CLT walls will be compromised, and the structure will collapse.

This comparison provides an example of how using too much exposed CLT or exposed mass timber in the compartment has grave consequences on the structural integrity of the components used.

#### 4.7 Exposed Timber vs. Decay Phase

The determination of decay phase was not in the scope of this research. Out of all the calculation methods mentioned in this study, only Xing et al. (2024) method provides an explanation of how exposed mass timber or CLT can influence the decay phase of a fire.

The concerns raised in Xing et al. (2024) about the decay phase of a fire is that the phenomenon of smoldering can occur during the decay phase of the fire. The smoldering temperature is less than that of the fire temperature. The smoldering process can lead to the continuous burning of the exposed structural components, even if the fire temperature at that instance is not enough to keep the fire burning (Xing et al., 2024).

Traditionally, to find the fire temperature during the decay phase, the formulas that are provided by EN 1991-1-2:2002 are mentioned by Xing et al. (2024, Equation 25). According to Xing et al. (2024), the formulas given in EN 1991-1-2:2002 do not correspond to actual temperatures during the decay phase. Therefore, these formulas underestimate fire temperatures.

The three-stage fire model by Xing et al. (2024) provides an equation for determining the fire temperature during the decay phase as follows (Xing et al., 2024, Equation 30):

$$\theta^{i+1} = -1500 \log\left(\frac{t^{i+1}}{t^i}\right) + \theta^i \quad (32)$$

In equation (32),  $t^i$  is the time when the average fire temperature inside the compartment is below 80% of the maximum fire temperature and  $\theta^i$  is the fire temperature at time  $t^i$ .

Unlike the equations of EN 1991-1-2:2002, which consider temperature calculation in terms of the time for the heating phase, to achieve maximum fire temperature  $t_{max}$ , leading to only one fire temperature in the decay phase, equation (32) provides the opportunity to calculate the fire temperature during the decay phase at any instance. This method of calculation of the decay phase will provide a more accurate representation of fire temperature when it comes to exposed CLT due to the following reasons:

- A higher fire load contribution leads to slower decay phase as the duration of fire is increased and combustion and smoldering phenomenon may continue in the compartment. In this case, equation (32) can be used to find fire temperature at any instance in the decay phase of the fire. The equations of EN 1991-1-2:2002 cannot adapt to this increase in fire load.
- Partially exposed surfaces in the compartment provide lesser fire load for fire temperature development, which leads to shorter fire durations and early burn-out in the compartment. The method of temperature determination during the decay phase by Xing et al. (2024), can facilitate in this scenario as well, while the equations of EN 1991-1-2:2002 cannot.

## 5. CONCLUSION

This thesis examined and compared four different design methods used for structural fire design of exposed mass timber and exposed CLT utilized in a fire compartment. The design methods utilized in this thesis were FprEN 1995-1-2-2023, Brandon (2018a, 2018b), Xing et al. (2024) and Salminen and Hietaniemi (2017). The focus of this thesis was to study how these different design methods model temperature development, charring behavior and contribution of fuel load when it comes to exposed timber elements in the compartment. The output parameters from these calculation methods provided insight into each calculation methodology where the parameters of the compartment were consistent for all calculation methods.

### 5.1 Results

Among the above-mentioned calculation methods, Salminen and Hietaniemi (2017) produced the highest peak fire temperature (1067 °C) but with the shortest fire duration (36.4 min), reason being that it considers the thermodynamic modeling of heat flux and air flow. This calculation method also produced the highest charring rate (1.01 mm/min) and the lowest charring depth (55 mm) out of all calculation methods. This emphasizes limited fuel load during the fire progression and ventilation driven burnout in the compartment.

The methods by Brandon (2018a, 2018b) and Xing et al. (2024) produced approximately similar fire durations (69.5 min and 69.4 min) and charring depths (86 mm and 85 mm). On the contrary, Xing et al. (2024) predicted a lower maximum fire temperature (977 °C) than Brandon (2018a, 2018b) (1059 °C), despite both methods utilizing the same fuel load contribution (156 MJ/m<sup>2</sup>). The lower charring rate of Xing et al. (2024) (0.81 mm/min) predicts a more gradual fire progression, which aligns better with this method's three-stage fire model.

The method included in FprEN 1995-1-2-2023 produced intermediate results with a relatively conservative charring depth (74 mm) and a relatively moderate fire temperature (1038 °C) compared to the other design methods. Although utilizing the same charring rate of 0.83 mm/min as Brandon (2018a, 2018b), the shorter fire duration (60 min) indicates that the assumptions of this method lead to lower results.

The results obtained from these calculation methods reinforce the fact that the selection of method is based on the context of the design application. FprEN 1995-1-2-2023 remains suitable for code-

compliant design. Brandon (2018a, 2018b) method offers a more practical approach with iterative corrections in regards of compartment specifications. Salminen and Hietaniemi (2017) method excels when it comes to accuracy, specifically in the case of performance based structural fire design by the utilization of heat flux and ventilation parameters. Xing et al. (2024) method bridges the gap between practical application and theoretical implications by simulating the fire progression using modified equations using its three-stage fire model.

Ultimately, there is not one right or wrong method when it comes to structural fire design. The choice of a particular design method is always based on the person performing the design and fire safety analysis. One thing that is needed to be considered is that the choice of design method should not be based only on ease of usage and how much the method is compliant with the code, but how well the calculation method predicts the expected behavior of fire in the structure and degree of precision needed in the structural fire design.

## **5.2 Further Research**

While this thesis has provided insight into the methodology and application of these different design approaches for fire design of exposed timber, there are opportunities for further research and development in this specific field of study.

Experimental validation of the calculation methods with full scale fire tests, especially in the case of exposed timber and CLT would provide a stronger foundation in understanding these calculation methods.

Integration of delamination when it comes to exposed CLT, specifically in the case of FprEN 1995-1-2-2023 and Brandon (2018a, 2018b), will lead to more precise and accurate results.

Developing more hybrid solutions to be applied in calculation methodologies. Combining the code compliance with the realism of thermodynamic modelling and parametric fire design, would bridge the gap between the practicality and accuracy of fire design using these calculation methods. Finally, expanding this analysis for multiple-room compartment and utilizing different ventilation configurations and different protective materials to promote limited exposure for fire load contribution, will promote practicality in the design where real fire scenarios are concerned. This will broaden the applicability of the findings from this research.

## REFERENCES

Arup.com. (2024). *Fire Safe Design of Mass Timber Buildings*. [online] Available at: <https://www.arup.com/insights/fire-safe-design-of-mass-timber-buildings/>.

Bartlett, A.I., Hadden, R.M. and Bisby, L.A. (2018). A Review of Factors Affecting the Burning Behaviour of Wood for Application to Tall Timber Construction. *Fire Technology*, 55(1), pp.1–49. doi:<https://doi.org/10.1007/s10694-018-0787-y>.

Brandon, D. (2016). Practical method to determine the contribution of structural timber to the rate of heat release and fire temperature of post-flashover compartment fires. *SP Arbetsrapport: 2016:68*, (ISSN 0284-5172).

Brandon D. (2018) Fire safety challenges of tall timber buildings – Phase 2: Task 4 - Engineering Methods. Report FRPF-2018-04. Quincy, MA: Fire Protection Research Foundation, 2018.

Buchanan, A. and Östman, B. (2022). *Fire Safe Use of Wood in Buildings*. Boca Raton: CRC Press. doi:<https://doi.org/10.1201/9781003190318>.

Dundar, U. and Selamet, S. (2022). Fire load and fire growth characteristics in modern high-rise buildings. *Fire Safety Journal*, 135, p.103710. doi:<https://doi.org/10.1016/j.firesaf.2022.103710>.

Fonseca, E.M.M. and Barreira, L.M.S. (2009). Charring rate determination of wood pine profiles submitted to high temperatures. *Safety and Security Engineering III*. doi:<https://doi.org/10.2495/safe090421>.

Frangi, A. and Fontana, M. (2005). Fire Performance Of Timber Structures Under Natural Fire Conditions. *Fire Safety Science*, 8, pp.279–290. doi:<https://doi.org/10.3801/iafss.fss.8-279>.

Gosselin, A., Blanchet, P., Lehoux, N. and Cimon, Y. (2016). Main Motivations and Barriers for Using Wood in Multi-Story and Non-Residential Construction Projects. *BioResources*, 12(1). doi:<https://doi.org/10.15376/biores.12.1.546-570>.

Harmathy, T.Z. (1972a). A new look at compartment fires, part I. *Fire Technology*, 8(3), pp.196–217. doi:<https://doi.org/10.1007/bf02590544>.

Harmathy, T.Z. (1972b). A new look at compartment fires, part II. *Fire Technology*, 8(4), pp.326–351. doi:<https://doi.org/10.1007/bf02590537>.

- Jozef Švajlenka and Terézia Pošiváková (2023). Innovation potential of wood constructions in the context of sustainability and efficiency of the construction industry. *Journal of Cleaner Production*, 411, pp.137209–137209. doi:<https://doi.org/10.1016/j.jclepro.2023.137209>.
- Kamyab, H., Klemeš, J.J., Fan, Y.V. and Lee, C.T. (2020). Transition to Sustainable Energy System for Smart Cities and Industries. *Energy*, 207, p.118104. doi:<https://doi.org/10.1016/j.energy.2020.118104>.
- Khelifa, M., Thi, V.D., Oudjène, M., Khennane, A., El Ganaoui, M. and Rogaume, Y. (2024). Modelling the Response of Timber Beams Under Fire. *International Journal of Civil Engineering*, 22(9), pp.1537–1549. doi:<https://doi.org/10.1007/s40999-024-00973-2>.
- Luc Girompaire and Dagenais, C. (2024). Fire Dynamics of Mass Timber Compartments with Exposed Surfaces: Development of an Analytical Model. *Fire technology*, 60(3). doi:<https://doi.org/10.1007/s10694-023-01528-y>.
- Maraveas, C., Miamis, K. and Matthaïou, Ch.E. (2013). Performance of Timber Connections Exposed to Fire: A Review. *Fire Technology*, 51(6), pp.1401–1432. doi:<https://doi.org/10.1007/s10694-013-0369-y>.
- Marcolan Júnior, A.C. and Dias de Moraes, P. (2018). Reliability on timber columns under fire situation. *Fire Research*. doi:<https://doi.org/10.4081/fire.2018.51>.
- Menis, A., Fragiaco, M. and Clemente, I. (2019). Fire resistance of unprotected cross-laminated timber floor panels: Parametric study and simplified design. *Fire Safety Journal*, 107, pp.104–113. doi:<https://doi.org/10.1016/j.firesaf.2018.02.001>.
- Ni, S. and Gernay, T. (2022). On the Effect of Exposed Timber on the Severity of Structural Fires in a Compartment and Required Firefighting Resources. *Fire Technology*, 58(5). doi:<https://doi.org/10.1007/s10694-022-01254-x>.
- Richter, F., Kotsovinos, P., Rackauskaite, E. and Rein, G. (2020). Thermal Response of Timber Slabs Exposed to Travelling Fires and Traditional Design Fires. *Fire Technology*, 57(1). doi:<https://doi.org/10.1007/s10694-020-01000-1>.
- Roza Aseeva, Serkov, B. and Andrey Sivenkov (2013a). Heat Release Characteristics and Combustion Heat of Timber. *Springer series in wood science*, pp.119–137. doi:[https://doi.org/10.1007/978-94-007-7460-5\\_5](https://doi.org/10.1007/978-94-007-7460-5_5).

Roza Aseeva, Serkov, B. and Andrey Sivenkov (2013b). Heat Release Characteristics and Combustion Heat of Timber. *Springer series in wood science*, pp.119–137. doi:[https://doi.org/10.1007/978-94-007-7460-5\\_5](https://doi.org/10.1007/978-94-007-7460-5_5).

Salminen, M. and J. Hietaniemi (2017). Performance-based fire design of a 14-story residential mass timber building. *CRC Press eBooks*, pp.53–62. doi:<https://doi.org/10.1201/9781315107202-7>.

Suzanne, M., Erez, G., Chaouchi, M., Bretonnet, C. and Thiry, A. (2023). Relationship between char depth of wood and cumulative heat exposure for fire investigation. *Fire Safety Journal*, [online] 140, p.103856. doi:<https://doi.org/10.1016/j.firesaf.2023.103856>.

Tran, H.C. and White, R.H. (1992). Burning rate of solid wood measured in a heat release rate calorimeter. *Fire and Materials*, 16(4), pp.197–206. doi:<https://doi.org/10.1002/fam.810160406>.

Viholainen, N., Kylkilahti, E., Autio, M. and Toppinen, A. (2020). A home made of wood: Consumer experiences of wooden building materials. *International Journal of Consumer Studies*, 44(6), pp.542–551. doi:<https://doi.org/10.1111/ijcs.12586>.

Xing, Z., Zhang, J. and Aslani, F. (2024). Theoretical model of the three - Stage parameter fire curve considering the contribution of combustible materials. *Journal of Building Engineering*, 94, pp.109903–109903. doi:<https://doi.org/10.1016/j.jobe.2024.109903>.

Yadav, R. and Kumar, J. (2022). Engineered Wood Products as a Sustainable Construction Material: A Review. *Engineered Wood Products for Construction*. doi:<https://doi.org/10.5772/intechopen.99597>.

**Annex A:****Calculations FprEN 1995-1-2:2023 method:****1) Input Parameters/ Initial Values, All 4 Walls Exposed:****1.1) Design Charring Rate:**

$$\beta_o := 0.65 \frac{mm}{min} \quad \text{FprEN 1995-1-2:2023, Table 5.4}$$

$$k_h := 1 \quad \text{FprEN 1995-1-2:2023, Table 5.3}$$

$$k_p := \sqrt{\frac{450}{380}} \quad \text{FprEN 1995-1-2:2023, Table 5.3. The value of 380 is taken as characteristic density of Spruce that is most commonly used in CLT in Finland.}$$

$$k_p = 1.088$$

$$\beta_n := k_h \cdot k_p \cdot \beta_o \quad \text{FprEN 1995-1-2:2023, Equation 5.2}$$

$$\beta_n = 0.707 \frac{mm}{min}$$

**1.2) Calculating the factor  $\Gamma$ :**

$$\rho := 470 \frac{kg}{m^3}$$

$$c := 1530 \frac{J}{kg \cdot K} \quad \text{FprEN 1995-1-2:2023, Table 8.1}$$

$$\lambda := 0.12 \frac{W}{m \cdot K} \quad \text{For 20 degrees temperature value. (Ambient Temperature)}$$

**1.3) Opening Factor:**

$$A_v := 1.85 \cdot 1.45$$

$$A_v = 2.683 \text{ m}^2$$

$$A_t := (2 \cdot 7 \cdot 2.9) + (2 \cdot 4 \cdot 2.9) + (2 \cdot 7 \cdot 4) - (1.85 \cdot 1.45) - (1 \cdot 2.13)$$

$$A_t = 114.988 \text{ m}^2 \quad \text{Total Area of the compartment excluding door and window}$$

$$h_{eq} := 1.45 \text{ m}$$

$$O := A_v \cdot \frac{\sqrt{h_{eq}}}{A_t} \quad \text{EN 1991-1-2:2024, Equation A.2}$$

$$O = 0.028 \quad m^{\frac{1}{2}}$$

Ranges between 0.02 and 0.20 so OK

$$\Gamma_1 := \frac{\left( \frac{O}{\sqrt{\rho \cdot c \cdot \lambda}} \right)^2}{\left( \frac{0.04}{1160} \right)^2}$$

EN 1991-1-2:2024, Equation A.2

$$\Gamma_1 = 7.691 \quad \frac{m \cdot s^5 \cdot K^2}{kg^2}$$

Now the design charring rate can be calculated from the following equation:

$$\beta_{par;1} := \beta_n \cdot \Gamma_1^{0.25}$$

FprEN 1995-1-2:2023, Equation A.9

$$\beta_{par;1} = 1.178 \quad \frac{mm}{min}$$

## 2) Iterations:

### 2.1) Iteration 1:

#### 2.1.1) Charring Depth:

$$A_f = 28 \quad m^2$$

$$A_t = 114.988 \quad m^2$$

$$q_{d;fi;t} := 550 \quad \frac{MJ}{m^2}$$

Value of fire load density related to floor area taken from (Buchanan & Östman, 2022)

$$q_{d;fi} := q_{d;fi;t} \cdot \frac{A_f}{A_t}$$

Design value of the fire load density related to the total surface area of the design fire compartment

$$q_{d;fi} = 133.928 \quad \frac{MJ}{m^2}$$

For first iteration, the design structural fire load density related to the total surface area of the design fire compartment is taken as zero

$$q_{d;st;t;1} := 0 \quad \frac{MJ}{m^2}$$

$$q_{d;total;f;1} := q_{d;fi;t} + q_{d;st;t;1}$$

FprEN 1995-1-2:2023, Equation A.12

$$q_{d;total;f;1} = 550 \quad \frac{MJ}{m^2}$$

$$q_{d;total;t;1} := q_{d;total;f;1} \cdot \frac{A_f}{A_t}$$

$$q_{d;total;t;1} = 133.928 \frac{MJ}{m^2}$$

The time at which a constant charring rate is assumed is taken from the following equation:

$$t_{o;1} := 0.009 \cdot \frac{q_{d;total;t;1}}{0} \quad \text{FprEN 1995-1-2:2023, Equation A,11}$$

$$t_{o;1} = 42.908 \quad \text{min}$$

The design charring depth, to determine the structural fire load for the next iteration, can be calculated using the following equation:

$$d_{char;t;1} := 2 \cdot \beta_{par;1} \cdot t_{o;1} \quad \text{FprEN 1995-1-2:2023, Equation A.10}$$

$$d_{char;t;1} = 101.086 \quad \text{mm}$$

## 2.2) Iteration 2:

### 2.2.1) Structural Fire Load:

$$m := 0.8 \quad \text{EN 1991-1-2:2024, Combustion Factor}$$

$$s_{10} := 0.12 \frac{MW}{m^2} \quad \text{FprEN 1995-1-2:2023, Equation A.13}$$

$$d_{char;t;1} = 101.086 \quad \text{mm} \quad \text{FprEN 1995-1-2:2023, Equation A.10}$$

$$\alpha_{st} := 1 \quad \text{FprEN 1995-1-2:2023, Equation A.13}$$

$$A_{st;1} := 57.167 \quad m^2 \quad \text{Area of Combusting Surfaces, 4 walls, excluding door and window}$$

$$q_{d;st;t;2} := 60 \cdot m \cdot s_{10} \cdot d_{char;t;1} \cdot \alpha_{st} \cdot \frac{A_{st;1}}{A_t} \quad \text{The design structural fire load density related to the total surface area of the design fire compartment}$$

$$q_{d;st;t;2} = 289.473 \frac{MJ}{m^2}$$

$$q_{d;total;f;2} := q_{d;fi;t} + 0.65 \cdot q_{d;st;t;2}$$

$$q_{d;total;f;2} = 738.157 \frac{MJ}{m^2}$$

$$q_{d;total;t;2} := q_{d;total;f;2} \cdot \frac{A_f}{A_t}$$

$$q_{d;total;t;2} = 179.745 \frac{MJ}{m^2}$$

FprEN 1995-1-2:2023, Equation A-12. The equation is adjusted for the modification that comes with the limitation that 70% of the fire is burning outside the compartment. This modification is valid when "to" is less than tmax. Meaning that the constant charring rate is achieved in the fully developed phase before the decay phase starts

### 2.2.2) Charring Depth:

$$t_{o,2} := 0.009 \cdot \frac{q_{d,total;t,2}}{O}$$

$$t_{o,2} = 57.587 \quad \text{min}$$

The design charring depth can be calculated using the following equation:

$$d_{char;t,2} := 2 \cdot \beta_{par;1} \cdot t_{o,2}$$

$$d_{char;t,2} = 135.668 \quad \text{mm}$$

### 2.3) Iteration 3:

#### 2.3.1) Structural Fire Load:

$$q_{d;st;t,3} := 60 \cdot m \cdot s_{10} \cdot d_{char;t,2} \cdot \alpha_{st} \cdot \frac{A_{st,1}}{A_t}$$

$$q_{d;st;t,3} = 388.502 \quad \frac{\text{MJ}}{\text{m}^2}$$

$$q_{d,total;f,3} := q_{d;fi,t} + 0.65 \cdot q_{d;st;t,3}$$

$$q_{d,total;f,3} = 802.527 \quad \frac{\text{MJ}}{\text{m}^2}$$

$$q_{d,total;t,3} := q_{d,total;f,3} \cdot \frac{A_f}{A_t}$$

$$q_{d,total;t,3} = 195.419 \quad \frac{\text{MJ}}{\text{m}^2}$$

#### 2.3.2) Charring Depth:

$$t_{o,3} := 0.009 \cdot \frac{q_{d,total;t,3}}{O}$$

$$t_{o,3} = 62.609 \quad \text{min}$$

The design charring depth can be calculated using the following equation:

$$d_{char;t,3} := 2 \cdot \beta_{par;1} \cdot t_{o,3}$$

$$d_{char;t,3} = 147.498 \quad \text{mm}$$

## 2.4) Iteration 4:

### 2.4.1) Structural Fire Load:

$$q_{d;st;t;4} := 60 \cdot m \cdot s_{10} \cdot d_{char;t;3} \cdot \alpha_{st} \cdot \frac{A_{st;1}}{A_t}$$

$$q_{d;st;t;4} = 422.381 \frac{MJ}{m^2}$$

$$q_{d;total;f;4} := q_{d;fi;t} + 0.65 \cdot q_{d;st;t;4}$$

$$q_{d;total;f;4} = 824.548 \frac{MJ}{m^2}$$

$$q_{d;total;t;4} := q_{d;total;f;4} \cdot \frac{A_f}{A_t}$$

$$q_{d;total;t;4} = 200.781 \frac{MJ}{m^2}$$

### 2.4.2) Charring Depth:

$$t_{o;4} := 0.009 \cdot \frac{q_{d;total;t;4}}{O}$$

$$t_{o;4} = 64.327 \text{ min}$$

The design charring depth can be calculated using the following equation:

$$d_{char;t;4} := 2 \cdot \beta_{par;1} \cdot t_{o;4}$$

$$d_{char;t;4} = 151.546 \text{ mm}$$

## 2.5) Iteration 5:

### 2.5.1) Structural Fire Load:

$$q_{d;st;t;5} := 60 \cdot m \cdot s_{10} \cdot d_{char;t;4} \cdot \alpha_{st} \cdot \frac{A_{st;1}}{A_t}$$

$$q_{d;st;t;5} = 433.971 \frac{MJ}{m^2}$$

$$q_{d;total;f;5} := q_{d;fi;t} + 0.65 \cdot q_{d;st;t;5}$$

$$q_{d;total;f;5} = 832.081 \frac{MJ}{m^2}$$

$$q_{d,total;t;5} := q_{d,total;f;5} \cdot \frac{A_f}{A_t}$$

$$q_{d,total;t;5} = 202.616 \frac{MJ}{m^2}$$

### 2.5.2) Charring Depth:

$$t_{o;5} := 0.009 \cdot \frac{q_{d,total;t;5}}{O}$$

$$t_{o;5} = 64.915 \text{ min}$$

The design charring depth can be calculated using the following equation:

$$d_{char;t;5} := 2 \cdot \beta_{par;1} \cdot t_{o;5}$$

$$d_{char;t;5} = 152.93 \text{ mm}$$

## 2.6) Iteration 6:

### 2.6.1) Structural Fire Load:

$$q_{d;st;t;6} := 60 \cdot m \cdot s_{10} \cdot d_{char;t;5} \cdot \alpha_{st} \cdot \frac{A_{st;1}}{A_t}$$

$$q_{d;st;t;6} = 437.936 \frac{MJ}{m^2}$$

$$q_{d,total;f;6} := q_{d;fi;t} + 0.65 \cdot q_{d;st;t;6}$$

$$q_{d,total;f;6} = 834.658 \frac{MJ}{m^2}$$

$$q_{d,total;t;6} := q_{d,total;f;6} \cdot \frac{A_f}{A_t}$$

$$q_{d,total;t;6} = 203.243 \frac{MJ}{m^2}$$

### 2.6.2) Charring Depth:

$$t_{o;6} := 0.009 \cdot \frac{q_{d,total;t;6}}{O}$$

$$t_{o;6} = 65.116 \text{ min}$$

The design charring depth can be calculated using the following equation:

$$d_{char;t;6} := 2 \cdot \beta_{par;1} \cdot t_{o;6}$$

$$d_{char;t;6} = 153.404 \text{ mm}$$

## 2.7) Iteration 7:

### 2.7.1) Structural Fire Load:

$$q_{d;st;t;7} := 60 \cdot m \cdot s_{10} \cdot d_{char;t;6} \cdot \alpha_{st} \cdot \frac{A_{st;1}}{A_t}$$

$$q_{d;st;t;7} = 439.292 \frac{MJ}{m^2}$$

$$q_{d;total;f;7} := q_{d;fi;t} + 0.65 \cdot q_{d;st;t;7}$$

$$q_{d;total;f;7} = 835.54 \frac{MJ}{m^2}$$

$$q_{d;total;t;7} := q_{d;total;f;7} \cdot \frac{A_f}{A_t}$$

$$q_{d;total;t;7} = 203.458 \frac{MJ}{m^2}$$

### 2.7.2) Charring Depth:

$$t_{o;7} := 0.009 \cdot \frac{q_{d;total;t;7}}{O}$$

$$t_{o;7} = 65.184 \text{ min}$$

The design charring depth can be calculated using the following equation:

$$d_{char;t;7} := 2 \cdot \beta_{par;1} \cdot t_{o;7}$$

$$d_{char;t;7} = 153.566 \text{ mm}$$

The criteria for stopping the iterations stated in the Eurocode is that the charring depth between consecutive iterations should not increase more than 0.5 mm. The increase of charring depth from Iteration 6 to 7 is 0.162 mm. Therefore, there is no need for further iterations.

### 2.7.3) Time for Fully Developed Phase:

$$t_{lim} := 0.33 \text{ h}$$

$$t_{max;7} := \max \left( 0.2 \cdot 10^{-3} \cdot \frac{q_{d;total;t;7}}{O}, t_{lim} \right) = 1.449 \text{ h} \quad \text{EN 1991-1-2:2024, Equation A.7}$$

### 2.7.4) Maximum Fire Temperature:

$$\theta_{max;5} := 20 + 1325 \left( 1 - 0.324 \cdot e^{-0.2 \cdot t_{max;7} \cdot \Gamma_1} - 0.204 \cdot e^{-1.7 \cdot t_{max;7} \cdot \Gamma_1} - 0.472 \cdot e^{-19 \cdot t_{max;7} \cdot \Gamma_1} \right)$$

$$\theta_{max;5} = 1298.75 \text{ } ^\circ\text{C}$$

EN 1991-1-2:2024, Equation A.1

From the analytical point of view, these iterations satisfy the criteria of convergence mentioned in the Eurocode, but consider this in a practical manner, the CLT thickness in the apartment is taken as 175 mm. The charring depth of 153.566 mm suggests that the structure will collapse which is not ideal when structural fire design is concerned. This calls for a change in the input parameters, reducing the exposed surface area to get safer design results.

### 3) Input Parameters/ Initial Values, One Wall Exposed (4m x 2.9m):

#### 3.1) Design Charring Rate:

The design charring rate will remain the same as it was in the previous case where all 4 walls were exposed.

#### 3.2) Calculating the factor $\Gamma$ :

Now, in this case 3 walls, the ceiling and the floor are protected. Two layers of 15.9 mm gypsum are used to protect the exposed surfaces. So there is a modification in the form of thermal factor that is calculated using the weighted surface area between the plasterboard and the exposed timber as mentioned in (Buchanan & Östman, 2022).

#### Timber Properties:

$$\rho_1 := 470 \frac{\text{kg}}{\text{m}^3}$$

$$c_1 := 1530 \frac{\text{J}}{\text{kg} \cdot \text{K}}$$

$$\lambda_1 := 0.12 \frac{\text{W}}{\text{m} \cdot \text{K}}$$

FprEN 1995-1-2:2023, Table 8.1

For 20 degrees temperature value. (Ambient Temperature)

$$A_{st;2} := 4 \cdot 2.9$$

Area of Combusting Surfaces

$$A_{st;2} = 11.6 \text{ } \text{m}^2$$

#### Gypsum Board Properties:

$$\rho_2 := 950 \frac{\text{kg}}{\text{m}^3}$$

$$c_2 := 960 \frac{\text{J}}{\text{kg} \cdot \text{K}}$$

FprEN 1995-1-2:2023, Table 8.2

$$\lambda_2 := 0.40 \frac{\text{W}}{\text{m} \cdot \text{K}}$$

For 20 degrees temperature value. (Ambient Temperature)

$$A_{prot} := (2 \cdot 7 \cdot 2.9) + (4 \cdot 2.9) + (2 \cdot 4 \cdot 7)$$

Area of Fire Protected Surfaces

$$A_{prot} = 108.2 \quad m^2$$

The thermal parameter, which is the weighted surface area between the exposed timber and the gypsum layers can be calculated as follow:

$$Ther_{par} := \frac{A_{st;2} \cdot \sqrt{\rho_1 \cdot c_1 \cdot \lambda_1} + A_{prot} \cdot \sqrt{\rho_2 \cdot c_2 \cdot \lambda_2}}{A_t}$$

$$Ther_{par} = 597.969$$

### 3.3) Opening Factor:

The opening factor will remain the same as in the case of previous calculations.

$$\Gamma_2 := \frac{\left( \frac{O}{Ther_{par}} \right)^2}{\left( \frac{0.04}{1160} \right)^2}$$

$$\Gamma_2 = 1.856 \quad \frac{m \cdot s^5 \cdot K^2}{kg^2}$$

Now the design charring rate can be calculated from the following equation:

$$\beta_{par;2} := \beta_n \cdot \Gamma_2^{0.25}$$

$$\beta_{par;2} = 0.826 \quad \frac{mm}{min}$$

### 4) Iterations:

#### 4.1) Iteration 8:

##### 4.1.1) Charring Depth:

$$q_{d,total;f;8} := q_{d;fi;t} + q_{d;st;t;1}$$

$$q_{d,total;f;8} = 550 \quad \frac{MJ}{m^2}$$

$$q_{d,total;t;8} := q_{d,total;f;8} \cdot \frac{A_f}{A_t}$$

$$q_{d,total;t;8} = 133.928 \quad \frac{MJ}{m^2}$$

The time at which a constant charring rate is assumed is taken from the following equation:

$$t_{o,8} := 0.009 \cdot \frac{q_{d;total;t,8}}{0}$$

$$t_{o,8} = 42.908 \quad \text{min}$$

The design charring depth, to determine the structural fire load for the next iteration, can be calculated using the following equation:

$$d_{char;t,8} := 2 \cdot \beta_{par,2} \cdot t_{o,8}$$

$$d_{char;t,8} = 70.851 \quad \text{mm}$$

## 4.2) Iteration 9:

### 4.2.1) Structural Fire Load:

Area of Combusting Surfaces, 4m x 2.9m  
wall

$$A_{st,2} = 11.6 \quad \text{m}^2$$

$$q_{d;st;t,9} := 60 \cdot m \cdot s_{10} \cdot d_{char;t,8} \cdot \alpha_{st} \cdot \frac{A_{st,2}}{A_t}$$

The design structural fire load density related to the total surface area of the design fire compartment

$$q_{d;st;t,9} = 41.169 \quad \frac{\text{MJ}}{\text{m}^2}$$

$$q_{d;total;f,9} := q_{d;fi;t} + 0.65 \cdot q_{d;st;t,9}$$

$$q_{d;total;f,9} = 576.76 \quad \frac{\text{MJ}}{\text{m}^2}$$

FprEN 1995-1-2:2023, Equation A-12. The equation is adjusted for the modification that comes with the limitation that 70% of the fire is burning outside the compartment. This modification is valid when to is less than tmax. Meaning that the constant charring rate is achieved in the fully developed phase before the decay phase starts

$$q_{d;total;t,9} := q_{d;total;f,9} \cdot \frac{A_f}{A_t}$$

$$q_{d;total;t,9} = 140.444 \quad \frac{\text{MJ}}{\text{m}^2}$$

### 4.2.2) Charring Depth:

$$t_{o,9} := 0.009 \cdot \frac{q_{d;total;t,9}}{0}$$

$$t_{o,9} = 44.996 \quad \text{min}$$

The design charring depth can be calculated using the following equation:

$$d_{char;t,9} := 2 \cdot \beta_{par,2} \cdot t_{o,9}$$

$$d_{char;t,9} = 74.298 \quad \text{mm}$$

### 4.3) Iteration 10:

#### 4.3.1) Structural Fire Load:

$$q_{d,st;t,10} := 60 \cdot m \cdot s_{10} \cdot d_{char;t,9} \cdot \alpha_{st} \cdot \frac{A_{st,2}}{A_t}$$

$$q_{d,st;t,10} = 43.172 \frac{MJ}{m^2}$$

$$q_{d,total;f,10} := q_{d;fi;t} + 0.65 \cdot q_{d,st;t,10}$$

$$q_{d,total;f,10} = 578.062 \frac{MJ}{m^2}$$

$$q_{d,total;t,10} := q_{d,total;f,10} \cdot \frac{A_f}{A_t}$$

$$q_{d,total;t,10} = 140.761 \frac{MJ}{m^2}$$

#### 4.3.2) Charring Depth:

$$t_{o,10} := 0.009 \cdot \frac{q_{d,total;t,10}}{O}$$

$$t_{o,10} = 45.097 \text{ min}$$

The design charring depth can be calculated using the following equation:

$$d_{char;t,10} := 2 \cdot \beta_{par;2} \cdot t_{o,10}$$

$$d_{char;t,10} = 74.466 \text{ mm}$$

### 4.4) Iteration 11:

#### 4.4.1) Structural Fire Load:

$$q_{d,st;t,11} := 60 \cdot m \cdot s_{10} \cdot d_{char;t,10} \cdot \alpha_{st} \cdot \frac{A_{st,2}}{A_t}$$

$$q_{d,st;t,11} = 43.27 \frac{MJ}{m^2}$$

$$q_{d,total;f,11} := q_{d;fi;t} + 0.65 \cdot q_{d,st;t,11}$$

$$q_{d,total;f,11} = 578.125 \frac{MJ}{m^2}$$

$$q_{d,total;t,11} := q_{d,total;f,11} \cdot \frac{A_f}{A_t}$$

$$q_{d;total;t;11} = 140.776 \frac{MJ}{m^2}$$

#### 4.4.2) Charring Depth:

$$t_{o;11} := 0.009 \cdot \frac{q_{d;total;t;11}}{O}$$

$$t_{o;11} = 45.102 \text{ min}$$

The design charring depth can be calculated using the following equation:

$$d_{char;t;11} := 2 \cdot \beta_{par;2} \cdot t_{o;11}$$

$$d_{char;t;11} = 74.474 \text{ mm}$$

#### 4.5) Iteration 12:

##### 4.5.1) Structural Fire Load:

$$q_{d;st;t;12} := 60 \cdot m \cdot s_{10} \cdot d_{char;t;11} \cdot \alpha_{st} \cdot \frac{A_{st;2}}{A_t}$$

$$q_{d;st;t;12} = 43.275 \frac{MJ}{m^2}$$

$$q_{d;total;f;12} := q_{d;fi;t} + 0.65 \cdot q_{d;st;t;12}$$

$$q_{d;total;f;12} = 578.128 \frac{MJ}{m^2}$$

$$q_{d;total;t;12} := q_{d;total;f;12} \cdot \frac{A_f}{A_t}$$

$$q_{d;total;t;12} = 140.777 \frac{MJ}{m^2}$$

##### 4.5.2) Charring Depth:

$$t_{o;12} := 0.009 \cdot \frac{q_{d;total;t;12}}{O}$$

$$t_{o;12} = 45.103 \text{ min}$$

The design charring depth can be calculated using the following equation:

$$d_{char;t;12} := 2 \cdot \beta_{par;2} \cdot t_{o;12}$$

$$d_{char;t;12} = 74.474 \text{ mm}$$

### 4.5.3) Time for Fully Developed Phase:

$$t_{max;12} := \max \left( 0.2 \cdot 10^{-3} \cdot \frac{q_{d;total;t;12}}{O}, t_{lim} \right) = 1.002 \text{ h}$$

### 4.5.4) Maximum Fire Temperature:

$$\theta_{max;12} := 20 + 1325 \left( 1 - 0.324 \cdot e^{-0.2 \cdot t_{max;12} \cdot \Gamma_2} - 0.204 \cdot e^{-1.7 \cdot t_{max;12} \cdot \Gamma_2} - 0.472 \cdot e^{-19 \cdot t_{max;12} \cdot \Gamma_2} \right)$$

$$\theta_{max;12} = 1037.636 \text{ } ^\circ\text{C}$$

The increase of charring depth from Iteration 4 to 5 is 0 mm, which means that conversion criteria is satisfied. Therefore, there is no need for further iterations.

Now, for the case of only one wall exposed to contribute towards the fire load inside the compartment, the final charring depth obtained is 74.474 mm. Considering the thickness of CLT is 175 mm, 44 % of the CLT is available to withstand the fire at the fully developed phase of the fire, which means that the structure will remain stable and will not collapse, which is desirable considering the structural fire design. The duration of fire is also within the acceptable range now.

## 5) Final Results:

### 3.1) Charring Rate:

$$\beta_{par} := 0.826 \frac{mm}{min}$$

### 3.2) Charring Depth:

$$d_{char} := 74.474 \text{ mm}$$

### 3.3) Maximum Time For Fully Developed Phase:

$$t_{max} := 1.002 \cdot 60 \text{ h}$$

$$t_{max} = 60.12 \text{ min}$$

### 3.4) Maximum Fire Load:

$$q_{td,max} := 140.777 \frac{MJ}{m^2}$$

### 3.5) Maximum Fire Temperature:

$$\theta_{max} := 1037.636 \text{ } ^\circ\text{C}$$

## Annex B:

### Calculations Brandon (2018a, 2018b) method:

#### 1) Input Parameters/ Initial Values:

##### 1.1) Moveable Fire Load:

The moveable fire load in the calculations is taken from (Buchanan & Östman, 2022), which provides a moveable fuel load of 550 MJ/m<sup>2</sup> in case of dwellings for the calculations using Brandon (2018a, 2018b) method.

$$A_f := 28 \text{ m}^2 \quad \text{Area of Floor}$$

$$A_t := 119.8 \text{ m}^2 \quad \text{Total Area of the Compartment}$$

$$q_{mf} := 550 \cdot \frac{A_f}{A_t} \quad \text{Moveable Fuel Load Per Unit Surface of the Compartment}$$

$$q_{mf} = 128.548 \frac{\text{MJ}}{\text{m}^2}$$

##### 1.2) Area of CLT:

The next thing to calculate is the area of exposed CLT. In the compartment, one wall (4m x 2.9m) is left exposed and the other three walls, the ceiling and floor is protected against fire. Then the area of CLT will be:

$$A_{CLT} := 4 \cdot 2.9$$

$$A_{CLT} = 11.6 \text{ m}^2$$

##### 1.3) Charring Depth:

$$\beta_\rho := 0.65 \frac{\text{mm}}{\text{min}} \quad \text{FprEN 1995-1-2:2023, Table 5.4}$$

$$k_h := 1 \quad \text{The thickness of CLT panel is assumed to be } > 20 \text{ mm, (175 mm)}$$

$$k_p := \sqrt{\frac{450}{380}} \quad \text{FprEN 1995-1-2:2023, Table 5.3. The value of 380 is taken as characteristic density of Spruce that is most commonly used in CLT in Finland}$$

$$k_p = 1.088$$

The notional design charring rate is calculated using following equation:

$$\beta_n := k_h \cdot k_p \cdot \beta_0$$

FprEN 1995-1-2:2023, Equation 5.2

$$\beta_n = 0.707 \frac{mm}{min}$$

#### 1.4) Calculating the factor $\Gamma$ :

In our case, 3 walls, the ceiling and the floor are protected. Two layers of 15.9 mm gypsum are used to protect the exposed surfaces. So there is a modification in the form of thermal factor that is calculated using the weighted surface area between the plaster board and the exposed timber as mentioned in (Buchanan & Östman, 2022).

#### Timber Properties:

$$\rho_1 := 470 \frac{kg}{m^3}$$

$$c_1 := 1530 \frac{J}{kg \cdot K}$$

$$\lambda_1 := 0.12 \frac{W}{m \cdot K}$$

FprEN 1995-1-2:2023, Table 8.1

For 20 degrees temperature value. (Ambient Temperature)

$$A_{st} := 4 \cdot 2.9$$

Area of Combusting Surfaces

$$A_{st} = 11.6 \quad m^2$$

#### Gypsum Board Properties:

$$\rho_2 := 950 \frac{kg}{m^3}$$

Brandon, (2018b), Table 4

$$c_2 := 960 \frac{J}{kg \cdot K}$$

Brandon, (2018b), Table 4

$$\lambda_2 := 0.40 \frac{W}{m \cdot K}$$

Brandon, (2018b), Table 4

$$A_{prot} := (2 \cdot 7 \cdot 2.9) + (4 \cdot 2.9) + (2 \cdot 4 \cdot 7)$$

Area of Fire Protected Surfaces

$$A_{prot} = 108.2 \quad m^2$$

The thermal parameter, which is the weighted surface area between the exposed timber and the gypsum layers can be calculated as follow:

$$Ther_{par} := \frac{A_{st} \cdot \sqrt{\rho_1 \cdot c_1 \cdot \lambda_1} + A_{prot} \cdot \sqrt{\rho_2 \cdot c_2 \cdot \lambda_2}}{A_t}$$

$$Ther_{par} = 573.948$$

The opening factor O can be calculated as follow:

$$A_v := 1.85 \cdot 1.45$$

$$A_v = 2.683 \text{ m}^2$$

$$h_v := 1.45 \text{ m}$$

$$O := \frac{A_v}{A_t} \cdot \sqrt{h_v}$$

Brandon, (2018b), Equation 3

$$O = 0.027 \text{ m}^{\frac{1}{2}}$$

$$\Gamma := \frac{\left( \frac{O}{\text{Ther}_{par}} \right)^2}{\left( \frac{0.04}{1160} \right)^2}$$

Brandon, (2018b), Equation 2

$$\Gamma = 1.856 \frac{\text{m} \cdot \text{s}^5 \cdot \text{K}^2}{\text{kg}^2}$$

### 1.5) Correction Factor:

The next value in the calculations is the correction factor " $\alpha_1$ " which provides correction for the boundary conditions in the compartment.

$$\alpha_1 := 5.39 \frac{\frac{\text{MJ}}{\text{m}^2}}{\text{mm}}$$

(Buchanan & Östman, 2022)

### 1.6) Charring Rate:

$$\beta_{par} := \beta_n \cdot \Gamma^{0.25}$$

Brandon, (2018b), Equation 9

$$\beta_{par} = 0.826 \frac{\text{mm}}{\text{min}}$$

## 2) Iterations:

### 2.1) Iteration 1:

$$t_{o;1} := 0.009 \cdot \frac{q_{mfl}}{O}$$

Brandon, (2018b), Equation 10

$$t_{o;1} = 42.908 \text{ min}$$

$$d_{char;end;1} := 2 \cdot \beta_{par} \cdot t_{o;1} \quad \text{Brandon, (2018b), Equation 13}$$

$$d_{char;end;1} = 70.851 \quad mm \quad \text{Design Charring Depth}$$

$$t_{lim} := 0.33 \quad h \quad \text{Limit Value for Medium Fire}$$

$$t_{max} := \max\left(0.2 \cdot 10^{-3} \cdot \frac{q_{mfl}}{O}, t_{lim}\right) \quad \text{Brandon, (2018b), Equation 4}$$

$$t_{max} = 0.954 \quad h$$

Now the final fuel load that includes the contribution of exposed timber can be calculated using the following equation mentioned below (Brandon, 2018b, Equation 16). Maximum time is multiplied by 60 to convert it into minutes and this value will remain constant throughout the iterations.

$$q_{td;1} := q_{mfl} + \frac{A_{CLT} \cdot \alpha_1 \cdot (d_{char;end;1} - (0.7 \cdot \beta_{par} \cdot t_{max} \cdot 60))}{A_t} \quad \text{Brandon, (2018b), Equation 16}$$

$$q_{td;1} = 148.269 \quad \frac{MJ}{m^2}$$

## 2.2) Iteration 2:

$$t_{o;2} := 0.009 \cdot \frac{q_{td;1}}{O}$$

$$t_{o;2} = 49.491 \quad min$$

$$d_{char;end;2} := 2 \cdot \beta_{par} \cdot t_{o;2}$$

$$d_{char;end;2} = 81.72 \quad mm$$

$$q_{td;2} := q_{mfl} + \frac{A_{CLT} \cdot \alpha_1 \cdot (d_{char;end;2} - (0.7 \cdot \beta_{par} \cdot t_{max} \cdot 60))}{A_t}$$

$$q_{td;2} = 153.942 \quad \frac{MJ}{m^2}$$

## 2.3) Iteration 3:

$$t_{o;3} := 0.009 \cdot \frac{q_{td;2}}{O}$$

$$t_{o;3} = 51.384 \quad min$$

$$d_{char;end;3} := 2 \cdot \beta_{par} \cdot t_{o;3}$$

$$d_{char;end;3} = 84.847 \quad mm$$

$$q_{td;3} := q_{mfl} + \frac{A_{CLT} \cdot \alpha_1 \cdot (d_{char;end;3} - (0.7 \cdot \beta_{par} \cdot t_{max} \cdot 60))}{A_t}$$

$$q_{td;3} = 155.573 \quad \frac{MJ}{m^2}$$

#### 2.4) Iteration 4:

$$t_{o;4} := 0.009 \cdot \frac{q_{td;3}}{O}$$

$$t_{o;4} = 51.929 \quad min$$

$$d_{char;end;4} := 2 \cdot \beta_{par} \cdot t_{o;4}$$

$$d_{char;end;4} = 85.746 \quad mm$$

$$q_{td;4} := q_{mfl} + \frac{A_{CLT} \cdot \alpha_1 \cdot (d_{char;end;4} - 0.7 \cdot \beta_{par} \cdot t_{max} \cdot 60)}{A_t}$$

$$q_{td;4} = 156.043 \quad \frac{MJ}{m^2}$$

#### 2.5) Iteration 5:

$$t_{o;5} := 0.009 \cdot \frac{q_{td;4}}{O}$$

$$t_{o;5} = 52.086 \quad min$$

$$d_{char;end;5} := 2 \cdot \beta_{par} \cdot t_{o;5}$$

$$d_{char;end;5} = 86.005 \quad mm$$

$$q_{td;5} := q_{mfl} + \frac{A_{CLT} \cdot \alpha_1 \cdot (d_{char;end;5} - (0.7 \cdot \beta_{par} \cdot t_{max} \cdot 60))}{A_t}$$

$$q_{td;5} = 156.178 \quad \frac{MJ}{m^2}$$

#### 2.6) Iteration 6:

$$t_{o;6} := 0.009 \cdot \frac{q_{td;5}}{O}$$

$$t_{o;6} = 52.131 \quad min$$

$$d_{char;end;6} := 2 \cdot \beta_{par} \cdot t_{o;6}$$

$$d_{char;end;6} = 86.079 \quad mm$$

$$q_{td;6} := q_{mfl} + \frac{A_{CLT} \cdot \alpha_1 \cdot (d_{char;end;6} - (0.7 \cdot \beta_{par} \cdot t_{max} \cdot 60))}{A_t}$$

$$q_{td;6} = 156.217 \quad \frac{MJ}{m^2}$$

### 2.7) Iteration 7:

$$t_{o;7} := 0.009 \cdot \frac{q_{td;6}}{O}$$

$$t_{o;7} = 52.144 \quad min$$

$$d_{char;end;7} := 2 \cdot \beta_{par} \cdot t_{o;7}$$

$$d_{char;end;7} = 86.101 \quad mm$$

$$q_{td;7} := q_{mfl} + \frac{A_{CLT} \cdot \alpha_1 \cdot (d_{char;end;7} - (0.7 \cdot \beta_{par} \cdot t_{max} \cdot 60))}{A_t}$$

$$q_{td;7} = 156.228 \quad \frac{MJ}{m^2}$$

### 2.8) Iteration 8:

$$t_{o;8} := 0.009 \cdot \frac{q_{td;7}}{O}$$

$$t_{o;8} = 52.148 \quad min$$

$$d_{char;end;8} := 2 \cdot \beta_{par} \cdot t_{o;8}$$

$$d_{char;end;8} = 86.107 \quad mm$$

$$q_{td;8} := q_{mfl} + \frac{A_{CLT} \cdot \alpha_1 \cdot (d_{char;end;8} - (0.7 \cdot \beta_{par} \cdot t_{max} \cdot 60))}{A_t}$$

$$q_{td;8} = 156.231 \quad \frac{MJ}{m^2}$$

### 2.9) Iteration 9:

$$t_{o;9} := 0.009 \cdot \frac{q_{td;8}}{O}$$

$$t_{o;9} = 52.149 \quad min$$

$$d_{char;end;9} := 2 \cdot \beta_{par} \cdot t_{o;9}$$

$$d_{char;end;9} = 86.109 \quad mm$$

$$q_{td;9} := q_{mfl} + \frac{A_{CLT} \cdot \alpha_1 \cdot (d_{char;end;9} - (0.7 \cdot \beta_{par} \cdot t_{max} \cdot 60))}{A_t}$$

$$q_{td;9} = 156.232 \quad \frac{MJ}{m^2}$$

### 2.10) Iteration 10:

$$t_{o;10} := 0.009 \cdot \frac{q_{td;9}}{O}$$

$$t_{o;10} = 52.149 \quad min$$

$$d_{char;end;10} := 2 \cdot \beta_{par} \cdot t_{o;10}$$

$$d_{char;end;10} = 86.109 \quad mm$$

$$q_{td;10} := q_{mfl} + \frac{A_{CLT} \cdot \alpha_1 \cdot (d_{char;end;10} - (0.7 \cdot \beta_{par} \cdot t_{max} \cdot 60))}{A_t}$$

$$q_{td;10} = 156.232 \quad \frac{MJ}{m^2}$$

As the iterations can be stopped now, we can find the final fire temperature and the maximum time for the fully developed phase of the fire.

$$t_{max;f} := \max \left( 0.2 \cdot 10^{-3} \cdot \frac{q_{td;10}}{O}, t_{lim} \right)$$

$$t_{max;f} = 1.159 \quad h$$

$$\theta_{max} := 20 + 1325 \left( 1 - 0.324 \cdot e^{-0.2 \cdot t_{max;f} \cdot \Gamma} - 0.204 \cdot e^{-1.7 \cdot t_{max;f} \cdot \Gamma} - 0.472 \cdot e^{-19 \cdot t_{max;f} \cdot \Gamma} \right)$$

$$\theta_{max} = 1058.807$$

Brandon, (2018b), Equation 1

### 3) Final Results:

There are two criteria mentioned in Brandon (2018a, 2018b) method for stopping the iterations.

-The difference between consecutive charring depths is < 0.1%.

-The duration of fully developed phase is so long that it is considered continuous, meaning the duration of the fire keeps on increasing.

In our calculations, the iterations 9 and 10 yields the same values of charring depth, meaning that the convergence is achieved and the difference is < 0.1%, So, the iterations can be stopped.

The Output Parameters are:

**3.1) Charring Rate:**

$$\beta_{par} = 0.826 \quad \frac{mm}{min}$$

**3.2) Charring Depth:**

$$d_{char} := 86.109 \quad mm$$

**3.3) Maximum Time For Fully Developed Phase:**

$$t_{max;final} := 1.159 \cdot 60$$

$$t_{max;final} = 69.54 \quad min$$

**3.4) Maximum Fire Load:**

$$q_{td;max} := 156.232 \quad \frac{MJ}{m^2}$$

**3.5) Maximum Fire Temperature:**

$$\theta_{max} = 1058.807 \quad ^\circ C$$

## Annex C:

### Calculations Xing et al. (2024) method:

#### 1) Input Parameters/ Initial Values:

##### 1.1) Exposed Charring Rate %:

$$exp := 10$$

This exp value represents the amount of exposed surface area in the compartment. In this case, one 4m x 2.9m wall contributes to 10 percent of the total exposed surface area in the compartment

$$\beta_{exp} := 29.66 - 47.51 \cdot 0.93^{exp}$$

Xing et al. (2024), Equation 1

$$\beta_{exp} = 6.666$$

This is the percentage of rate of increase of charring rate to the exposed area of CLT

##### 1.2) Heating Rate Factor $\Gamma$ :

$$\Gamma := 1.856 \frac{m \cdot s^5 \cdot K^2}{kg^2}$$

Calculated in Brandon (2018a, 2018b) method

##### 1.3) Design Charring Rate:

$$\beta_o := 0.65 \frac{mm}{min}$$

FprEN 1995-1-2:2023, Table 5.4

##### 1.4) Parametric Fire Charring Rate:

$$\beta_{par} := 1.5 \cdot \beta_o \cdot \frac{0.2 \cdot \sqrt{\Gamma} - 0.04}{0.16 \cdot \sqrt{\Gamma} + 0.08} \cdot (1 + (0.01 \cdot \beta_{exp}))$$

Xing et al. (2024), Equation 2

$$\beta_{par} = 0.811 \frac{mm}{min}$$

##### 1.5) Fire Load for the Calculations:

This method suggests using the fire load that is calculated using Brandon (2018a, 2018b) method. Those values are already calculated, I will take the final value of fire load that was obtained after iterations.

$$q_{td} := 156.232 \frac{MJ}{m^2}$$

Calculated in Brandon (2018a, 2018b) method

## 2) Calculations:

### 2.1) Charring Depth:

$$O := 0.027 \text{ m}^{\frac{1}{2}}$$

Calculated in Brandon (2018a, 2018b)  
method

$$t_0 := 0.009 \cdot \frac{q_{td}}{O}$$

Xing et al. (2024), Equation 24

$$t_0 = 52.077 \text{ min}$$

$$d_{char} := 2 \cdot \beta_{par} \cdot t_0$$

Xing et al. (2024), Equation 25

$$d_{char} = 84.507 \text{ mm}$$

### 2.2) Maximum Time For Fully Developed Phase:

$$A_t := (2 \cdot 7 \cdot 2.9) + (2 \cdot 4 \cdot 2.9) + (2 \cdot 7 \cdot 4)$$

$$A_t = 119.8 \text{ m}^2$$

$$A_f := 7 \cdot 4$$

$$A_f = 28 \text{ m}^2$$

$$t_{lim} := 0.33 \text{ h}$$

Limit Value for Medium Fire

$$t_{max} := \max\left(0.2 \cdot 10^{-3} \cdot \frac{q_{td}}{O}, t_{lim}\right)$$

Xing et al. (2024), Equation 23

$$t_{max} = 1.157 \text{ h}$$

### 2.3) Maximum Fire Temperature Using Parametric Fire:

$$\theta_{max} := 20 + 1325 \left(1 - 0.324 \cdot e^{-0.2 \cdot t_{max} \cdot \Gamma} - 0.204 \cdot e^{-1.7 \cdot t_{max} \cdot \Gamma} - 0.472 \cdot e^{-19 \cdot t_{max} \cdot \Gamma}\right)$$

$$\theta_{max} = 1058.604 \text{ }^\circ\text{C}$$

Xing et al. (2024), Equation 20

### 2.4) Maximum Fire Temperature using Xing's Equation:

$$\Omega := \frac{(119.8 - 2.683)}{2.683 \cdot \sqrt{1.5}}$$

Xing et al. (2024), Equation 16

$$\Omega = 35.641$$

$$T_g := 6000 \cdot \frac{(1 - e^{-0.1 \cdot \Omega})}{\sqrt{\Omega}}$$

Xing et al. (2024), Equation 15

$$T_g = 976.556 \text{ } ^\circ\text{C}$$

### Verifying the Convergence Criteria for these fire Temperatures:

$$\text{Convergence} := \left| \frac{T_g - \theta_{max}}{\theta_{max}} \right| \leq 10\%$$

Xing et al. (2024), Equation 27

$$\text{Convergence}_f = 7.7\%$$

The criteria state that this convergence value should be less than 10%. As the criteria is clearly satisfied, therefore, there is no need to perform iterations.

### 3) Final Results:

#### 3.1) Charring Rate:

$$\beta_{par} = 0.811 \frac{mm}{min}$$

#### 3.2) Charring Depth:

$$d_{char} = 84.507 \text{ } mm$$

#### 3.3) Maximum Time For Fully Developed Phase:

$$t_{max,f} = 1.157 \cdot 60 \text{ } h$$

$$t_{max,f} = 69.42 \text{ } min$$

#### 3.4) Maximum Fire Load:

$$q_{td} = 156.232 \frac{MJ}{m^2}$$

#### 3.5) Maximum Fire Temperature:

$$\theta_{max,f} = 976.556 \text{ } ^\circ\text{C}$$

**Annex D:****Calculations Salminen and Hietaniemi (2017) method:****1) Input Parameters/ Initial Values:**

The dimensions of the compartment are 7m x 4m.

Compartment Height is 2.9m

Size of Window is 1.85m x 1.45m

Size of Door is 1m x 2.13m

$$A_t := 119.18 \quad m^2 \quad \text{Total Area of the compartment}$$

$$A_w := 2.683 \quad m^2 \quad \text{Area of the Window}$$

$$A_f := 11.6 \quad m^2 \quad \text{Area in the Compartment that will contribute in the fire}$$

$$\alpha := 1 \quad \text{Variable Quantity}$$

$$A_{fz} := \alpha \cdot A_f \quad \text{Total Free Surface Area for Fire Contribution}$$

$$A_{fz} = 11.6 \quad m^2$$

$$c_g := 1100 \quad \frac{J}{kg \cdot K} \quad \text{Specific Heat of Air}$$

**1.1) Mass of CLT:**

The area of CLT wall of 4m x 2.9m is 11.6 metres square. Multiplying this value with the assumed thickness of 175 mm or 0.175 m. Multiplying both of these values will provide us with the volume of CLT which is 2.03 metre cube. Now multiplying this value with the assumed density of CLT to be 470 kg/metres cube we get the mass of CLT.

$$G_o := 954.1 \quad kg \quad \text{Mass of CLT}$$

**1.2) Ventilation Parameter:**

$$\rho := 1.293 \quad \frac{kg}{m^3} \quad \text{Density of Air}$$

$$a := 0.7$$

$$g := 9.8 \quad \frac{m}{s^2} \quad \text{Acceleration Due to Gravity}$$

$h := 1.45 \text{ m}$  Height of Opening

$\phi := \rho \cdot a \cdot g^{\frac{1}{2}} \cdot A_w \cdot h^{\frac{1}{2}}$  Ventilation Parameter

$\phi = 9.154 \frac{\text{kg}}{\text{s}}$  Harmathy (1972a), Equation 16

### 1.3) Flame Height:

$l := 0.75 \cdot A_f^{\frac{1}{3}}$  Harmathy (1972a), Equation 38b

$l = 1.698 \text{ m}$  Flame Height

### 1.4) Flow Rate of Air:

$U_a := 0.145 \cdot \phi$  Harmathy (1972a), Equation 17

$U_{a,f} := 2.29 \frac{\text{kg}}{\text{s}}$  Flow Rate of Air, Entering from lower one third of window area

### 1.5) Rate of Change of Fuel Mass:

$R := 0.0062 \cdot A_f$  Harmathy (1972a), Equation 28a

$R = 0.072 \frac{\text{kg}}{\text{s}}$  Rate of change of mass of fuel

### 1.6) Other Input Values:

$\beta := 1$  Constant

$\zeta := 1.05$  Constant

$\eta := 0.9$  Constant

$T_o := 20 \text{ }^\circ\text{C}$  Temperature at time t=0 or Ambient Temperature

$k_c := 0.15 \frac{\text{J}}{\text{m} \cdot \text{s} \cdot \text{K}}$  Thermal Conductivity of Linning Material

$k_d := 0.12 \cdot 10^{-6} \frac{\text{m}^2}{\text{s}}$  Thermal Diffusivity of Linning Material

$\sigma := 5.67 \cdot 10^{-8} \frac{\text{W}}{\text{m}^2 \cdot \text{K}^4}$  Stefan-Boltzmann Constant

$\Delta H_c := 26 \cdot 10^6 \frac{\text{J}}{\text{kg}}$  Heat of Combustion for Char Layer

$$\Delta H_v := 15 \cdot 10^6 \frac{J}{kg}$$

Heat of Combustion of Volatile Gases

## 2) Calculations:

### 2.1) Time for Primary Fire Development:

$$\tau := \frac{151}{\frac{A_f}{G_o}}$$

Harmathy (1972b), Equation 44a

$$\tau = 12419.75 \text{ s}$$

Time of Primary Burning

### 2.2) Calculating the Maximum Temperature:

To calculate the maximum temperature, the procedure that is proposed in the Harmathy (1972a, 1972b) literature is to assume a temperature first and then calculate a quantity known as effective heat flux and then use that quantity to calculate the maximum temperature. Repeat the procedure to get more accurate values.

#### 2.2.1) Iteration 1:

The maximum temperature assumed is 900 degree celcius.

$$T_{assumed} := 900 \text{ } ^\circ C$$

The Effective Heat Flux can be calculated using the following formula:

$$q_{E,1} := \frac{1}{A_t} \cdot \left( R \cdot (0.932 \cdot \beta \cdot \Delta H_v - 0.068 \cdot \Delta H_c) - (U_{a,t} \cdot R) \cdot c_g \cdot (\zeta \cdot T_{assumed} - T_o) - \sigma \cdot \frac{A_w}{3} \cdot (T_{assumed}^4 - T_o^4) \right)$$

$$|q_{E,1}| = 5684.159 \frac{J}{m^2 \cdot s}$$

Harmathy (1972b), Equation 51

The maximum temperature can be calculated using the following formula:

$$T_{g,1} := \left( \frac{q_{E,1}}{\sigma \cdot \eta} + \left( T_o + \left( \sqrt{2} \cdot \frac{q_{E,1}}{k_c} \cdot \left( \frac{k_d \cdot \tau}{\pi} \right)^{\frac{1}{2}} \right) \right)^4 \right)^{\frac{1}{4}}$$

Gas Temperature

$$T_{g,1} = 1203.547 \text{ } ^\circ C$$

Harmathy (1972b), Equation 61

#### 2.2.2) Iteration 2:

$$T_{g,1,K} := T_{g,1} = 1203.547 \text{ } ^\circ C$$

The Effective Heat Flux can be calculated using the following formula:

$$q_{E,2} := \frac{1}{A_t} \cdot \left( R \cdot (0.932 \cdot \beta \cdot \Delta H_v - 0.068 \cdot \Delta H_c) - (U_{a,t} \cdot R) \cdot c_g \cdot (\zeta \cdot T_{g,1,K} - T_o) - \sigma \cdot \frac{A_w}{3} \cdot (T_{g,1,K}^4 - T_o^4) \right)$$

$$|q_{E;2}| = 4586.07 \frac{J}{m^2 \cdot s}$$

Now, the maximum temperature can be calculated using the following formula:

$$T_{g;2} := \left( \frac{|q_{E;2}|}{\sigma \cdot \eta} + \left( T_o + \left( \sqrt{2} \cdot \frac{q_{E;2}}{k_c} \cdot \left( \frac{k_d \cdot \tau}{\pi} \right)^{\frac{1}{2}} \right) \right)^4 \right)^{\frac{1}{4}}$$

$$T_{g;2} = 986.07 \text{ } ^\circ\text{C}$$

### 2.2.3) Iteration 3:

$$T_{g;2;K} := T_{g;2} = 986.07 \text{ } ^\circ\text{C}$$

The Effective Heat Flux can be calculated using the following formula:

$$q_{E;3} := \frac{1}{A_t} \cdot \left( |R| \cdot (0.932 \cdot \beta \cdot \Delta H_v - 0.068 \cdot \Delta H_c) - (U_{a,t} \cdot |R|) \cdot |c_g| \cdot (\zeta \cdot T_{g;2;K} - T_o) - \sigma \cdot \frac{A_w}{3} \cdot (T_{g;2;K}^4 - T_o^4) \right)$$

$$|q_{E;3}| = 5423.676 \frac{J}{m^2 \cdot s}$$

Now, the maximum temperature can be calculated using the following formula:

$$T_{g;3} := \left( \frac{q_{E;3}}{\sigma \cdot \eta} + \left( T_o + \left( \sqrt{2} \cdot \frac{q_{E;3}}{k_c} \cdot \left( \frac{k_d \cdot \tau}{\pi} \right)^{\frac{1}{2}} \right) \right)^4 \right)^{\frac{1}{4}}$$

$$T_{g;3} = 1151.563 \text{ } ^\circ\text{C}$$

### 2.2.4) Iteration 4:

$$T_{g;3;K} := T_{g;3} = 1151.563 \text{ } ^\circ\text{C}$$

The Effective Heat Flux can be calculated using the following formula:

$$q_{E;4} := \frac{1}{A_t} \cdot \left( |R| \cdot (0.932 \cdot \beta \cdot \Delta H_v - 0.068 \cdot \Delta H_c) - (U_{a,t} \cdot |R|) \cdot |c_g| \cdot (\zeta \cdot T_{g;3;K} - T_o) - \sigma \cdot \frac{A_w}{3} \cdot (T_{g;3;K}^4 - T_o^4) \right)$$

$$|q_{E;4}| = 4813.571 \frac{J}{m^2 \cdot s}$$

Now, the maximum temperature can be calculated using the following formula:

$$T_{g,4} := \left( \frac{q_{E,4}}{\sigma \cdot \eta} + \left( T_o + \left( \sqrt{2} \cdot \frac{q_{E,4}}{k_c} \cdot \left( \frac{k_d \cdot \tau}{\pi} \right)^{\frac{1}{2}} \right) \right)^4 \right)^{\frac{1}{4}}$$

$$T_{g,4} = 1030.715 \quad ^\circ\text{C}$$

### 2.2.5) Iteration 5:

$$T_{g,4;K} := T_{g,4} = 1030.715 \quad ^\circ\text{C}$$

The Effective Heat Flux can be calculated using the following formula:

$$q_{E,5} := \frac{1}{A_t} \cdot \left( |R| \cdot (0.932 \cdot \beta \cdot \Delta H_v - 0.068 \cdot \Delta H_c) - (U_{a,t} \cdot |R|) \cdot |c_g| \cdot (\zeta \cdot T_{g,4;K} - T_o) - \sigma \cdot \frac{A_w}{3} \cdot (T_{g,4;K}^4 - T_o^4) \right)$$

$$|q_{E,5}| = 5274.467 \frac{J}{m^2 \cdot s}$$

Now, the maximum temperature can be calculated using the following formula:

$$T_{g,5} := \left( \frac{q_{E,5}}{\sigma \cdot \eta} + \left( T_o + \left( \sqrt{2} \cdot \frac{q_{E,5}}{k_c} \cdot \left( \frac{k_d \cdot \tau}{\pi} \right)^{\frac{1}{2}} \right) \right)^4 \right)^{\frac{1}{4}}$$

$$T_{g,5} = 1121.88 \quad ^\circ\text{C}$$

### 2.2.6) Iteration 6:

$$T_{g,5;K} := T_{g,5} = 1121.88 \quad ^\circ\text{C}$$

The Effective Heat Flux can be calculated using the following formula:

$$q_{E,6} := \frac{1}{A_t} \cdot \left( |R| \cdot (0.932 \cdot \beta \cdot \Delta H_v - 0.068 \cdot \Delta H_c) - (U_{a,t} \cdot |R|) \cdot |c_g| \cdot (\zeta \cdot T_{g,5;K} - T_o) - \sigma \cdot \frac{A_w}{3} \cdot (T_{g,5;K}^4 - T_o^4) \right)$$

$$|q_{E,6}| = 4935.162 \frac{J}{m^2 \cdot s}$$

Now, the maximum temperature can be calculated using the following formula:

$$T_{g,6} := \left( \frac{q_{E,6}}{\sigma \cdot \eta} + \left( T_o + \left( \sqrt{2} \cdot \frac{q_{E,6}}{k_c} \cdot \left( \frac{k_d \cdot \tau}{\pi} \right)^{\frac{1}{2}} \right) \right)^4 \right)^{\frac{1}{4}}$$

$$T_{g,6} = 1054.68 \text{ } ^\circ\text{C}$$

### 2.2.7) Iteration 7:

$$T_{g,6;K} := T_{g,6} = 1054.68 \text{ } K$$

The Effective Heat Flux can be calculated using the following formula:

$$q_{E,7} := \frac{1}{A_t} \cdot \left( |R| \cdot (0.932 \cdot \beta \cdot \Delta H_v - 0.068 \cdot \Delta H_c) - (U_{a,t} \cdot |R|) \cdot |c_g| \cdot (\zeta \cdot T_{g,6;K} - T_o) - \sigma \cdot \frac{A_w}{3} \cdot (T_{g,6;K}^4 - T_o^4) \right)$$

$$|q_{E,7}| = 5189.973 \frac{J}{m^2 \cdot s}$$

Now, the maximum temperature can be calculated using the following formula:

$$T_{g,7} := \left( \frac{q_{E,7}}{\sigma \cdot \eta} + \left( T_o + \left( \sqrt{2} \cdot \frac{q_{E,7}}{k_c} \cdot \left( \frac{k_d \cdot \tau}{\pi} \right)^{\frac{1}{2}} \right) \right)^4 \right)^{\frac{1}{4}}$$

$$T_{g,7} = 1105.105 \text{ } ^\circ\text{C}$$

### 2.2.8) Iteration 8:

$$T_{g,7;K} := T_{g,7} = 1105.105 \text{ } ^\circ\text{C}$$

The Effective Heat Flux can be calculated using the following formula:

$$q_{E,8} := \frac{1}{A_t} \cdot \left( |R| \cdot (0.932 \cdot \beta \cdot \Delta H_v - 0.068 \cdot \Delta H_c) - (U_{a,t} \cdot |R|) \cdot |c_g| \cdot (\zeta \cdot T_{g,7;K} - T_o) - \sigma \cdot \frac{A_w}{3} \cdot (T_{g,7;K}^4 - T_o^4) \right)$$

$$|q_{E,8}| = 5001.355 \frac{J}{m^2 \cdot s}$$

Now, the maximum temperature can be calculated using the following formula:

$$T_{g,8} := \left( \frac{q_{E,8}}{\sigma \cdot \eta} + \left( T_o + \left( \sqrt{2} \cdot \frac{q_{E,8}}{k_c} \cdot \left( \frac{k_d \cdot \tau}{\pi} \right)^{\frac{1}{2}} \right) \right)^4 \right)^{\frac{1}{4}}$$

$$T_{g,8} = 1067.754 \text{ } ^\circ\text{C}$$

### 2.2.9) Final Result For Temperature:

The calculations present a general idea of how the change in heat flux is generating fire temperatures inside the compartment. The idea presented in the paper mentioned that the purpose of iterations was to follow the trend of the temperature to predict more accurate values. The iterations suggest that the difference between subsequent iterations keep on decreasing and the temperature values are converging, i.e. the values are becoming more accurate. The value of Iteration 8 presents the least difference between the subsequent iterations therefore this value is considered the accurate and final value of temperature.

$$T_{max} := T_{g,8} = 1067.754 \text{ } ^\circ\text{C}$$

### 2.3) Maximum Time for Fully Developed Phase:

The time  $\tau$  calculated previously that suggests the time for primary burning of fire, is the time that represents the totality of the fully developed phase, rather the  $t_{max}$  value which represents the time at which the peak temperature is attained. Therefore, to get the  $t_{max}$  value, the formula from Eurocode can be used:

$$q_{td} := \frac{G_o}{A_{fz}} \quad \text{Harmathy (1972b)}$$

$$q_{td} = 82.25 \frac{\text{kg}}{\text{m}^2}$$

$$O := A_w \cdot \frac{\sqrt{h}}{A_t} \quad \text{Opening Factor}$$

$$O = 0.027 \text{ } \frac{1}{\text{m}^2}$$

Ranges between 0.02 and 0.20 so OK

$$t_{lim} := 0.33 \text{ } h$$

$$t_{max} := \max\left(0.2 \cdot 10^{-3} \cdot \frac{q_{td}}{O}, t_{lim}\right) = 0.607 \text{ } h \quad \text{EN 1991-1-2:2024, Equation A-7}$$

### 2.4) Charring Rate:

The charring rate will be calculated using equations from the Eurocode:

$$\beta_o := 0.65 \frac{\text{mm}}{\text{min}} \quad \text{FprEN 1995-1-2:2023, Table 5.4}$$

$$k_h := 1 \quad \text{FprEN 1995-1-2:2023, Table 5.3}$$

$$k_p := \sqrt{\frac{450}{380}} \quad \text{FprEN 1995-1-2:2023, Table 5.3. The value of 380 is taken as characteristic density of Spruce that is most commonly used in CLT in Finland}$$

$$k_p = 1.088$$

$$\beta_n := k_h \cdot k_p \cdot \beta_o$$

FprEN 1995-1-2:2023, Equation 5.2

$$\beta_n = 0.707 \frac{mm}{min}$$

Nominal Charring Rate

$$\rho_2 := 550 \frac{kg}{m^3}$$

Density of Wood, (Harmathy, 1972a, 1972b)

$$c := 2300 \frac{J}{kg \cdot K}$$

Specific Heat of Wood, Harmathy (1972b)

$$\lambda := 0.12 \frac{W}{m \cdot K}$$

For 20 degrees temperature value, Ambient Temperature

$$\Gamma := \frac{\left( \frac{O}{\sqrt{\rho_2 \cdot c \cdot \lambda}} \right)^2}{\left( \frac{0.04}{1160} \right)^2}$$

EN 1991-1-2:2024, Equation A.2

$$\Gamma = 4.071 \frac{m \cdot s^5 \cdot K^2}{kg^2}$$

Now the design charring rate can be calculated from the following equation:

$$\beta_{par} := \beta_n \cdot \Gamma^{0.25}$$

FprEN 1995-1-2:2023, Equation A.9

$$\beta_{par} = 1.005 \frac{mm}{min}$$

## 2.5) Calculating Charring Depth:

$$q_{td} = 82.25 \frac{MJ}{m^2}$$

The time at which a constant charring rate is assumed is taken from the following equation:

$$t_o := 0.009 \cdot \frac{q_{td}}{O}$$

FprEN 1995-1-2:2023, Equation A.11

$$t_o = 27.307 \text{ min}$$

The design charring depth can be calculated using the following equation:

$$d_{char} := 2 \cdot \beta_{par} \cdot t_o$$

FprEN 1995-1-2:2023, Equation A.10

$$d_{char} = 54.874 \text{ mm}$$

**3) Final Results:****3.1) Charring Rate:**

$$\beta_{par} = 1.005 \quad \frac{mm}{min}$$

**3.2) Charring Depth:**

$$d_{char} = 54.874 \quad mm$$

**3.3) Maximum Time For Fully Developed Phase:**

$$t_{max,t} := 0.607 \cdot 60 \quad h$$

$$t_{max,t} = 36.42 \quad min$$

**3.4) Maximum Fire Load:**

$$q_{td,max} := 82.25 \quad \frac{MJ}{m^2}$$

**3.5) Maximum Fire Temperature:**

$$T_{max} = 1067.754 \quad ^\circ C$$